

Coupled Dyson-Schwinger Equations and Effects of Self-Consistency

S. S. Wu, H. X. Zhang, Y. J. Yao

Center for Theoretical Physics and Department of Physics
Jilin University, Changchun 130023
People's Republic of China

Abstract

Using the $\sigma - \omega$ model as an effective tool, the effects of self-consistency are studied in some detail. A coupled set of Dyson-Schwinger equations for the renormalized baryon and meson propagators in the $\sigma - \omega$ model is solved self-consistently according to the dressed Hartree-Fock scheme, where the hadron propagators in both the baryon and meson self-energies are required to also satisfy this coupled set of equations. It is found that the self-consistency affects the baryon spectral function noticeably, if only the interaction with σ mesons is considered. However, there is a cancellation between the effects due to the σ and ω mesons and the additional contribution of ω mesons makes the above effect insignificant. In both the σ and $\sigma - \omega$ cases the effects of self-consistency on meson spectral function are perceptible, but they can nevertheless be taken account of without a self-consistent calculation. Our study indicates that to include the meson propagators in the self-consistency requirement is unnecessary and one can stop at an early step of an iteration procedure to obtain a good approximation to the fully self-consistent results of all the hadron propagators in the model, if an appropriate initial input is chosen. Vertex corrections and their effects on ghost poles are also studied.

PACS :21. 60 J_z, 21. 65. +f, 11. 10. Gh.

Keywords : Dyson-Schwinger Equations, effects of self-consistency.

1 . Introduction

For a strong coupling theory it is important to go beyond the perturbation calculation. The Dyson-Schwinger (DS) equation provides one of the effective means to achieve such a goal. As is wellknown, the requirement of self-consistency can make the infinite series of Feynman diagrams contained in the solution to the equation nested, with each nest again containing the same infinite series of nested diagrams. However, the equation will then become nonlinear and not easy to solve. There is always the question what new effects on the solution may be produced by such a nesting and whether the latter is always important. In the zero-density case Brown, Puff and Wilets [1] as well as Bielajew and Serot [2] have solved the DS equation for the renormalized baryon propagators self-consistently according to the dressed Hartree-Fock (HF) scheme. As is wellknown, the $\sigma - \omega$ model has achieved considerable success in the description of many bulk and single particle properties of nuclei [3]. Thus it is worthwhile to use it as a tool to study the effect of self-consistency in some detail. For simplicity we shall only consider the case of zero-density, where the tadpole self-energies need not be taken into account. The different self-consistent (dressed) HF schemes are illustrated in Fig. 1. By "dressed" it is meant that in the baryon and meson self-energies the hadron propagators are not all bare. If one requires self-consistency in the baryon propagators, i.e. $\overline{G} = G$ in Fig. 1a, while sets $\overline{\Delta} = \Delta^0$ and $\overline{D} = D^0$, it is referred to as scheme BP. In this case the DS equation represented by Fig. 1a is already closed. Since $\overline{G} = G$, it is easily seen by iteration that the self-energy is now nested and the nesting repeats again and again. Clearly one may also require self-consistency in all the hadron propagators contained in the self-energies. This implies that one should have $\overline{G} = G$, $\overline{\Delta} = \Delta$ and $\overline{D} = D$ and it will be referred to as the fully self-consistent (FSC) scheme. In order to solve for G , Δ and D we must now consider a coupled set of DS equations, since the propagators are mutually correlated as shown in Fig. 1. Such a set of equations has been solved recently by Bracco, Eiras, Krein and Wilets (BEKW) [4] for a $\pi - \omega$ model. Their calculation shows that the effect of self-consistency on the spectral properties of the hadron propagators is not significant and it also can not make the ghost poles disappear. Following previous works by Milana [5], Allendes and Serot [6] and Krein, Nielsen, Puff and Wilets [7], BEKW further found that the ghost poles in all the hadron propagators considered in the model can be eliminated if vertex corrections are properly taken into account. Recently, by means of a simple model we have shown [8] that the self-consistency in scheme BP diminishes the continuum part of the spectral representation for the baryon propagator and for the calculation of the latter,

there is a simpler scheme which is a good approximation to scheme BP. We would like to ascertain whether the above results hold more generally. We shall study the coupled set of DS equations according to the FSC scheme. The effects of self-consistency will be investigated in some detail. It is found that they affect the baryon spectral function noticeably, in case only the σ meson is considered. However, there is almost no difference between the results obtained from scheme BP and FSC. It is interesting to find that the additional contribution of ω mesons makes the above effect insignificant. This indicates that there is a cancellation between the contributions from the σ and ω mesons. In both the σ and $\sigma - \omega$ cases the effects of self-consistency on meson spectral functions are perceptible, but they can be taken account of without a self-consistent calculation. Our calculation shows that to include the meson propagators in the self-consistent requirement is unnecessary and one can stop at an early step of an iteration procedure to obtain a good approximation to the FSC scheme for the calculation of all the hadron propagators in the model. In analogy to Ref. [4], we have also obtained that neither scheme BP nor scheme FSC can eliminate the ghost poles. Since the question of ghost poles is of vital theoretical importance, following Refs. [4, 6, 7, 9], we have further calculated the contributions of vertex corrections and studied their consequences. As both the ω and σ mesons are taken into account, vertex functions are only expressed by phenomenological form factors.

In Section 2 we shall consider the coupled set of DS equations for the renormalized hadron propagators in the $\sigma - \omega$ model and its reduction. The numerical results are given and discussed in Section 3. The vertex corrections and their consequences are studied in Section 4. Concluding remarks are presented in Section 5.

2 . The model and coupled Dyson-Schwinger equations

The Lagrangian density for the $\sigma - \omega$ model [3] is given by

$$L = -\bar{\psi}(\gamma_\mu \partial_\mu + M)\psi - \frac{1}{2}(\partial_\mu \phi \partial_\mu \phi + m_s^2 \phi^2) - \frac{1}{4}F_{\mu\nu}F_{\mu\nu} - \frac{1}{2}m_v^2 A_\mu A_\mu + g_s \bar{\psi}\psi\phi + ig_v \bar{\psi}\gamma_\mu \psi A_\mu + L_{CTC}, \quad (1)$$

where $F_{\mu\nu} = \partial_\mu A_\nu - \partial_\nu A_\mu$, $\partial_\mu = \frac{\partial}{\partial x_\mu}$, $x_\mu = (\vec{x}, ix_0)$, $x^2 = x_\mu x_\mu = \vec{x}^2 - x_0^2$ with $x_0 \equiv t$ and CTC means the counterterm correction introduced for the purpose of renormalization. The baryon, σ and ω meson propagators are

designated as follows:

$$G_{\alpha\beta}(x = x_1 - x_2) = \langle T[\psi_\alpha(x_1)\psi_\beta(x_2)] \rangle = \int \frac{d^4k}{(2\pi)^4} e^{ik_\rho x_\rho} G_{\alpha\beta}(k), \quad (2)$$

$$\Delta(x) = \langle T[\phi(x_1)\phi(x_2)] \rangle = \int \frac{d^4k}{(2\pi)^4} e^{ik_\rho x_\rho} \Delta(k), \quad (3)$$

$$D_{\mu\nu}(x) = \langle T[A_\mu(x_1)A_\nu(x_2)] \rangle = \int \frac{d^4k}{(2\pi)^4} e^{ik_\rho x_\rho} D_{\mu\nu}(k), \quad (4)$$

where $\langle 0 \rangle \equiv \langle \bar{\Psi}_0 | 0 | \bar{\Psi}_0 \rangle$ and $|\bar{\Psi}_0\rangle$ denotes the exact ground state. We note that our definition differs from the usual one by a factor of i . It is wellknown that the relevant DS equations in the dressed HF scheme (Fig. 1) can be written in the following form:

(a) for baryon

$$G(k) = G^0(k) + G^0(k)\Sigma(k)G(k) = -[\gamma_\mu k_\mu - iM + \Sigma(k)]^{-1}, \quad (5)$$

$$\Sigma(k) = \Sigma_s(k) + \Sigma_v(k), \quad (6a)$$

$$\Sigma_s(k) = -g_s^2 \int \frac{d^7q}{(2\pi)^4} \bar{G}(q) \bar{\Delta}_s(k-q) \Gamma_s(k, q, k-q) + \Sigma_{CTC}^s(k), \quad (6b)$$

$$\Sigma_v(k) = g_v^2 \int \frac{d^7q}{(2\pi)^4} \gamma_\eta \bar{G}(q) \bar{D}_{\eta\lambda}(k-q) \Gamma_\lambda(k, q, k-q) + \Sigma_{CTC}^v(k); \quad (6c)$$

(b) for σ -meson

$$\Delta_s(k) = \Delta_s^0(k) + \Delta_s^0(k)\Pi_s(k)\Delta_s(k) = -i[k^2 + m_s^2 + i\Pi_s(k) - i\epsilon]^{-1}, \quad (7)$$

$$\Pi_s(k) = g_s^2 \int \frac{d^7q}{(2\pi)^4} Tr[\bar{G}(k+q)\Gamma_s(k+q, q, k)\bar{G}(q)] + \Pi_{CTC}^s(k); \quad (8)$$

(c) for ω -meson

$$D_{\mu\nu}(k) = D_{\mu\nu}^0(k) + D_{\mu\eta}^0(k)\Pi_{\eta\lambda}(k)D_{\lambda\nu}(k), \quad (9)$$

$$\hat{\Pi}_{\eta\lambda}(k) = -g_v^2 \int \frac{d^7q}{(2\pi)^4} Tr[\gamma_\eta \bar{G}(k+q)\Gamma_\lambda(k+q, q, k)\bar{G}(q)]; \quad (10)$$

where Γ_s and Γ_λ are the σ -baryon and ω -baryon vertex functions, respectively (denoted by a heavy dot in Fig. 1), a caret indicates that the quantity is not yet renormalized, $\tau = 4 - \delta$ ($\delta \rightarrow 0^+$) and in Eq. (5) the Feynman prescription $M \rightarrow M - i\epsilon$ is understood. In this section vertex corrections

will not be considered, thus $\Gamma_s(p, q, k) = 1$ and $\Gamma_\lambda(p, q, k) = \gamma_\lambda$. Since the baryon current is conserved, we have

$$\widehat{\Pi}_{\mu\nu}(k) = \left(\delta_{\mu\nu} - \frac{k_\mu k_\nu}{k^2}\right)\widehat{\Pi}_v(k), \quad (11)$$

which implies $\widehat{\Pi}_v(k) = \frac{1}{3}\sum_\mu \widehat{\Pi}_{\mu\mu}(k)$. From Eq. (11) one observes that the renormalized $\Pi_{\mu\nu}(k)$ can be obtained from

$$\Pi_v(k) = \widehat{\Pi}_v(k) + \Pi_{CTC}^v(k). \quad (12)$$

To fix the renormalization counterterms we shall use the following conditions

$$\Sigma_\alpha(k) |_{\gamma_\mu k_\mu = iM_t} = 0; \quad \frac{\partial}{\partial(\gamma_\mu k_\mu)} \Sigma_\alpha(k) |_{\gamma_\mu k_\mu = iM_t} = 0, \quad (13a)$$

$$\Pi_\alpha(k) |_{k^2=0} = 0; \quad \frac{\partial}{\partial(k^2)} \Pi_\alpha(k) |_{k^2=0} = 0, \quad (13b)$$

where $\alpha = s$ or v and M_t denotes the true baryon mass. If we set $\overline{G} = G$, $\overline{\Delta}_s = \Delta_s$ and $\overline{D}_{\eta\lambda} = D_{\eta\lambda}$ in Eqs. (6, 8 and 10), it is seen that Eqs. (5-10) constitute a self-consistent closed set of DS equations for all the hadron propagators considered in the model. It thus yields the FSC scheme. We note that $D_{\eta\lambda}$ can be written as [10, 11]

$$D_{\eta\lambda}(k) = \left(\delta_{\eta\lambda} - \frac{k_\eta k_\lambda}{k^2}\right) \frac{-i}{k^2 + m_v^2 + i\Pi_v(k) - i\epsilon} - i \frac{k_\eta k_\lambda}{k^2(m_v^2 + \delta m_v^2)}, \quad (14)$$

where δm_v^2 is the mass counterterm for the ω -meson. Since the ω -meson couples to the conserved baryon current, we may set $D_{\eta\lambda} = \delta_{\eta\lambda}\Delta_v$ in Eq. (6c), where according to Eq. (14) Δ_v is given by

$$\Delta_v(k) = \Delta_v^0(k) + \Delta_v^0(k)\Pi_v(k)\Delta_v(k) = -i[k^2 + m_v^2 + i\Pi_v(k) - i\epsilon]^{-1}, \quad (15)$$

If we put $\overline{\Delta}_s = \Delta_s^0$ and $\overline{D}_{\eta\lambda} = D_{\eta\lambda}^0$ and only require $\overline{G} = G$, Eqs. (5) and (6) already build a closed self-consistent set, which has been called scheme BP. It is known that the original HF approximation to $G(k)$ is given by

$$G_\Sigma^0(k) = -[\gamma_\mu k_\mu - iM + \Sigma(\vec{k}, E_k)]^{-1}, \quad (16)$$

and the corresponding eigenvalue equation has the form

$$[\gamma_\mu k_\mu - iM + \Sigma(k)]_{k_0=E_k} u(k_s) = 0. \quad (17)$$

If in addition to the approximations $\bar{\Delta}_s = \Delta_s^0$ and $\bar{D}_{\eta\lambda} = \delta_{\eta\lambda}\Delta_v^0$, we further substitute G_Σ^0 for G in Eq. (6), we obtain

$$\Sigma(k) = \int \frac{d^4q}{(2\pi)^4} [-g_s^2 G_\Sigma^0(q) \Delta_s^0(k-q) + g_v^2 \gamma_\eta G_\Sigma^0(q) \gamma_\eta \Delta_v^0(k-q)] + \Sigma_{CTC}(k), \quad (18)$$

Setting $k_0 = E_k$ in Eq. (18), one obtains the self-consistent equation for the HF potential $\Sigma(\vec{k}, E_k) \equiv \Sigma(k)|_{k_0=E_k}$ [12]. Let the self-energy determined by Eq. (18) be indicated by a subscript p . We note that $G_p(k) = -[\gamma_\mu k_\mu - iM + \Sigma_p(k)]^{-1}$ is different from $G_\Sigma^0(k)$, because $\Sigma_p(k)$ is defined for all \vec{k} and k_0 , though $\Sigma_p(k)|_{k_0=E_k} = \Sigma(\vec{k}, E_k)$. It has been shown in Ref. [8] that $G_p(k)$ is a better approximation to $G(k)$ determined by scheme BP than $G_\Sigma^0(k)$ and such an approximation has been denoted as scheme P. Using G_p we shall show that there is an extended potential scheme which yields a good approximation to the FSC scheme for the calculation of all the hadron propagators in the model. The four-dimensional integrals involved in Eqs. (6, 8, 10) can be calculated by means of the spectral representation [1]. Following Ref. [2], we shall apply Feynman's integral parameterization to simplify the integration and use the standard method employed in the dimensional regularization to evaluate the relevant integrals. As is wellknown [13, 11], a properly normalized spectral representation for the baryon propagator may be expressed in the form

$$\tilde{G}(k) = -Z_2 \frac{\gamma_\mu k_\mu + iM_t}{k^2 + M_t^2 - i\epsilon} - \int_{m_1^2}^{\infty} dm^2 \frac{\gamma_\mu k_\mu \alpha(-m^2, Z_2) + iM_t \beta(-m^2, Z_2)}{k^2 + m^2 - i\epsilon}, \quad (19a)$$

where $m_1 = M_t + m_s$ and Z_2 satisfies

$$Z_2 + \int_{m_1^2}^{\infty} dm^2 \alpha(-m^2, Z_2) = 1; \quad (19b)$$

whereas for the meson propagators we have

$$\tilde{\Delta}_\lambda(k) = Z_\lambda \frac{-i}{k^2 + \tilde{m}_\lambda^2 - i\epsilon} - i \int_{th_\lambda}^{\infty} dm^2 \frac{\rho_\lambda(-m^2, Z_\lambda)}{k^2 + m^2 - i\epsilon}, \quad (20a)$$

where \tilde{m}_λ is the true meson mass, $\lambda = s$ or v , th_λ means the threshold where the continuum starts and

$$Z_\lambda + \int_{th_\lambda}^{\infty} dm^2 \rho_\lambda(-m^2, Z_\lambda) = 1. \quad (20b)$$

Since in Eq. (1) we have only considered the linear meson interaction and no meson self-interactions are included, from Eqs. (8) and (10) it is easily seen

that $th_\lambda = (2M_t)^2$. Comparing Eq. (19a) with Eq. (5) and Eq. (20a) with Eq. (7) as well as (15), we have $\tilde{G}(k) = ZG(k)$ and $\tilde{\Delta}_\lambda(k) = Y_\lambda\Delta_\lambda(k)$, where Z and Y_λ are proportional factors. It is not difficult to see that $Z_2 = ZZ_t$ where $(-Z_t)$ is the residue of $G(k)$ at the pole $\gamma_\mu k_\mu = iM_t$, while under the on-shell renormalization condition (13a) one has $Z_t = 1$ and $M = M_t$ [8]. Similarly, for the meson propagators $Z_\lambda = Y_\lambda R_\lambda$, where $(-iR_\lambda)$ is the residue of $\Delta_\lambda(k)$ at the pole $k^2 = -\tilde{m}_\lambda^2$. Denote the denominator of $\Delta_\lambda(k)$ by $D_\lambda(k^2)$ (Π_λ is a function of only k^2). The pole $(-\tilde{m}_\lambda^2)$ should clearly satisfy $D_\lambda(-\tilde{m}_\lambda^2) = 0$. From $D_\lambda(k^2) = D_\lambda(-\tilde{m}_\lambda^2) + (k^2 + \tilde{m}_\lambda^2)[\frac{dD_\lambda}{dk^2}]_{k^2=-\tilde{m}_\lambda^2} + \dots$, one finds immediately

$$R_\lambda = [1 + i(\partial\Pi_\lambda/\partial k^2)_{k^2=-\tilde{m}_\lambda^2}]^{-1}. \quad (21)$$

It is known [2] that in the zero-density case one may write

$$\Sigma(k) = \gamma_\mu k_\mu a(k^2) - iMb(k^2). \quad (22)$$

Denote $a = a_s + a_v$ and $b = b_s + b_v$. Substituting

$$\overline{G}(k) = Z^{-1}\tilde{G}(k) = -\int_0^\infty d\sigma^2 \frac{\gamma_\mu k_\mu f_\alpha(-\sigma^2) + iM_t f_\beta(-\sigma^2)}{k^2 + \sigma^2 - i\epsilon}, \quad (23a)$$

$$f_\gamma(-\sigma^2) = \delta(\sigma^2 - M_t^2) + \theta(\sigma^2 - m_1^2)\gamma(-\sigma^2), \quad (\gamma = \alpha \text{ or } \beta) \quad (23b)$$

$$\overline{\Delta}_\lambda(k) = Y_\lambda^{-1}\tilde{\Delta}_\lambda(k) = -i\int_0^\infty dm^2 \frac{h_\lambda(-m^2)}{k^2 + m^2 - i\epsilon}, \quad (23c)$$

$$h_\lambda(-m^2) = R_\lambda\delta(m^2 - \tilde{m}_\lambda^2) + \theta(m^2 - th_\lambda)\rho_\lambda(-m^2), \quad (\lambda = s \text{ or } v) \quad (23d)$$

into Eq. (6) and following the procedure suggested in Ref. [2], one easily finds

$$a_s(k^2) = \frac{g_s^2}{16\pi^2} \iint_0^\infty d\sigma^2 dm^2 \int_0^1 dx f_\alpha(-\sigma^2) h_s(-m^2) x \ln \frac{K^2(-M_t^2)}{K^2(k^2)} + c_s, \quad (24a)$$

$$b_s(k^2) = \frac{g_s^2}{16\pi^2} \iint_0^\infty d\sigma^2 dm^2 \int_0^1 dx f_\beta(-\sigma^2) h_s(-m^2) \ln \frac{K^2(k^2)}{K^2(-M_t^2)} + c_s, \quad (24b)$$

$$c_s = -\frac{g_s^2}{8\pi^2} M_t^2 \iint_0^\infty d\sigma^2 dm^2 \int_0^1 dx \frac{x(1-x)[x f_\alpha(-\sigma^2) + f_\beta(-\sigma^2)] h_s(-m^2)}{K^2(-M_t^2)}, \quad (24c)$$

$$K^2(k^2) \equiv K^2(x, \sigma^2, m^2, k^2) = x(1-x)k^2 + (1-x)\sigma^2 + xm^2; \quad (24d)$$

$$a_v(k^2) = \frac{g_v^2}{8\pi^2} \iint_0^\infty d\sigma^2 dm^2 \int_0^1 dx f_\alpha(-\sigma^2) h_v(-m^2) x \ln \frac{K^2(-M_t^2)}{K^2(k^2)} + c_v, \quad (25a)$$

$$b_v(k^2) = \frac{g_v^2}{4\pi^2} \iint_0^\infty d\sigma^2 dm^2 \int_0^1 dx f_\beta(-\sigma^2) h_v(-m^2) \ln \frac{K^2(-M_t^2)}{K^2(k^2)} + c_v, \quad (25b)$$

$$c_v = \frac{g_v^2}{4\pi^2} M_t^2 \iint_0^\infty d\sigma^2 dm^2 \int_0^1 dx \frac{x(1-x)[2f_\beta(-\sigma^2) - x f_\alpha(-\sigma^2)] h_v(-m^2)}{K^2(-M_t^2)}, \quad (25c)$$

where $\gamma(-\sigma^2) = Z^{-1}\gamma(-\sigma^2, Z_2)$, $\rho_\lambda(-m^2) = Y_\lambda^{-1}\rho_\lambda(-m^2, Z_\lambda)$ and

$$\alpha(k^2) = \frac{1}{\pi} \text{Im} \left[\frac{1 + a_s(k^2) + a_v(k^2)}{D(k^2)} \right], \quad (26a)$$

$$\beta(k^2) = \frac{1}{\pi} \text{Im} \left[\frac{1 + b_s(k^2) + b_v(k^2)}{D(k^2)} \right], \quad (26b)$$

$$D(k^2) = (1 + a_s(k^2) + a_v(k^2))^2 k^2 + (1 + b_s(k^2) + b_v(k^2))^2 M_t^2. \quad (26c)$$

It is seen that $h_\lambda(-m^2)$ is yet unknown and use must now be made of Eqs. (7-10). Since Eqs. (8) and (10) can be worked out in the same way, let us consider the latter. Substituting Eqs. (23a and b) into Eq. (10) and using the Feynman formula $(AB)^{-1} = \int_0^\infty dx [xA + (1-x)B]^{-2}$, one gets

$$\Sigma_\eta \hat{\Pi}_{\eta\eta}(k) = 8g_v^2 \iint_0^\infty d\sigma^2 dm^2 \int_0^1 dx \int \frac{d^r Q}{(2\pi)^4} \left[(Q^2 - x(1-x)k^2) F_\alpha(\sigma^2 m^2) + 2M_t^2 F_\beta(\sigma^2 m^2) \right] [Q^2 + K^2(k^2)]^{-2}, \quad (27)$$

where $F_\gamma(\sigma^2 m^2) = f_\gamma(-\sigma^2) f_\gamma(-m^2)$. By means of Eq. (13b) and the integration formula familiar in the dimensional regularization we obtain that

$$\begin{aligned} \Pi_v(k^2) &= \frac{1}{3} \Sigma_\eta [\hat{\Pi}_{\eta\eta}(k^2) - \hat{\Pi}_{\eta\eta}(0) - k^2 (\partial \hat{\Pi}_{\eta\eta} / \partial k^2)_{k^2=0}] \\ &= i \frac{g_v^2}{3\pi^2} \iint_0^\infty d\sigma^2 dm^2 \int_0^1 dx \{ [(K^2(k^2) + \frac{1}{2}x(1-x)k^2) F_\alpha(\sigma^2 m^2) - \\ &M_t^2 F_\beta(\sigma^2 m^2)] \ln \frac{K^2(k^2)}{K^2(0)} - x(1-x)k^2 [F_\alpha(\sigma^2 m^2) - \frac{M_t^2}{K^2(0)} F_\beta(\sigma^2 m^2)] \}, \end{aligned} \quad (28)$$

where the counterterms are supplied by terms $\frac{1}{2}\delta m_v^2 A_\mu A_\mu$ and $\varsigma_v \frac{1}{4} F_{\mu\nu} F_{\mu\nu}$ contained in L_{CTC} [see Eq. (1)]. Similarly we have

$$\begin{aligned} \Pi_s(k^2) &= i \frac{g_s^2}{4\pi^2} \iint_0^\infty d\sigma^2 dm^2 \int_0^1 dx \{ [(2K^2(k^2) + x(1-x)k^2) F_\alpha(\sigma^2 m^2) + \\ &M_t^2 F_\beta(\sigma^2 m^2)] \ln \frac{K^2(k^2)}{K^2(0)} - x(1-x)k^2 [2F_\alpha(\sigma^2 m^2) + \frac{M_t^2}{K^2(0)} F_\beta(\sigma^2 m^2)] \}. \end{aligned} \quad (29)$$

Further, using Eqs. (7, 15, 20) and the formula $(x - i\epsilon)^{-1} = \frac{P}{x} + i\pi\delta(x)$, we obtain

$$\rho_\alpha(k^2) = \frac{1}{\pi} \text{Im}[i\Delta_\alpha(k^2)], \quad (30)$$

for $k^2 < -th_\lambda$. Eqs. (24-26) and (28-30) are the explicit expressions for the closed set of renormalized DS equations used for the calculation. We note that through the renormalization conditions (13a and b) $G(k)$ and $\Delta_\alpha(k)$ given by Eqs.(5, 7, 15) are normalized differently from $\tilde{G}(k)$ and $\tilde{\Delta}_\lambda(k)$, respectively. According to Eqs. (19b) and (20b) we shall define I_b (I_λ) given below

$$I_b \equiv Z \int_{m_1^2}^{\infty} dm^2 \alpha(-m^2) = 1 - ZZ_t, \quad (19c)$$

$$I_\lambda \equiv Y_\lambda \int_{th_\lambda}^{\infty} dm^2 \rho_\lambda(-m^2) = 1 - Y_\lambda R_\lambda, \quad (20c)$$

as the impurity factor of the single particle (sp) character of a baryon (λ -meson). Clearly, it just tells the relative importance of the continuum part.

3 . Numerical results

Though the set of self-consistent DS equations for scheme FSC obtained in Section 2 looks somewhat formidable, it can be solved rigorously and quite easily by the method of iteration. Thus, it provides a useful example for the study of self-consistency and diagram nesting. In the following the mass values used are $M_t = 4.7585$, $m_s = 2.6353$ and $m_v = 3.9680(fm^{-1})$. We shall first consider the case of baryons interacting only with σ mesons. Two values of the strength parameter $\bar{g}_s^2 (\equiv \frac{g_s^2}{16\pi^2})$ are studied. Since the results of $\bar{g}_s^2 = 0.5263$ and 0.6517 display the same qualitative behavior, only the former will be represented graphically. From Figs. 2 and 3 one sees that the results obtained from schemes BP and FSC are almost the same. Let us denote a physical quantity $Q(k)$ by $Q(k; S)$ or simply $Q(S)$, if it is calculated according to scheme S . Though one has set $\bar{\Delta}_s = \Delta_s^0$ in scheme BP, one may substitute the baryon propagator $G(k; BP)$ obtained from it into Eq. (8) and find $\rho_s(k^2; BP)$ from Eq. (30). It is found that $\rho_s(k^2; BP)$ and $\rho_s(k^2; FSC)$ are very close to each other. Thus, only the latter is shown in Fig. 4. The above results indicate that to include the meson propagators in the self-consistency requirement may not be necessary. Form Eqs. (5-10) it is seen that all the self-energies will be known, if \bar{G} , $\bar{\Delta}_s$ and $\bar{D}_{\eta\lambda}$ are known. Thus different approximate schemes are obtained, if different choices are made for \bar{G} , $\bar{\Delta}_s$ and $\bar{D}_{\eta\lambda}$. To assess the importance of self-consistency and to ask whether one may stop at an earlier step of the iteration process, we have

shown in Fig. 3 results from five different calculation schemes which are explained in Table 1. The first column gives the name of each scheme, while the second and third explain how its Σ_s [Σ_v] and Π_s [Π_v] are obtained from Eqs. (6b) [(6c)] and (8) [(10)], respectively. For instance, $\Sigma_s(P)$ and $\Pi_s(P)$ in scheme P are obtained by setting $\overline{G} = G_\Sigma^0$, $\overline{\Delta}_s = \Delta_s^0$ in Eq. (6b) and $\overline{G} = G_\Sigma^0$ in Eq. (8), $\Sigma_s(PEP)$ and $\Pi_s(PEP)$ in the partially extended P scheme (PEP) by $\overline{G} = G(P)$, $\overline{\Delta}_s = \Delta_s^0$ in Eq. (6b) and $\overline{G} = G(P)$ in Eq. (8), whereas to obtain $\Sigma_s(EP)$ and $\Pi_s(EP)$ for the extended P scheme (EP), one sets $\overline{G} = G(P)$, $\overline{\Delta}_s = \Delta_s(P)$ in Eq. (6b) and $\overline{G} = G(P)$ in Eq. (8), etc. The quantities in the brackets are for ω -mesons in the $\sigma - \omega$ model. From Fig. 3 it is seen that the self-consistency diminishes the continuum part of the spectral representation for the baryon propagator [8], though the convergent process from $(\alpha(P), \beta(P))$ to $(\alpha(FSC), \beta(FSC))$ is oscillatory. It is interesting to note that the contribution of the meson self-consistency, though very small, adds toward the same direction. Clearly we have

$$\begin{aligned} \alpha(PEP) &\simeq \alpha(EP), & \beta(PEP) &\simeq \beta(EP) \\ \alpha(BP) &\simeq \alpha(FSC), & \beta(BP) &\simeq \beta(FSC) \end{aligned} \quad , \quad (31a)$$

whereas Fig. 4 shows

$$\rho_s(PEP) = \rho_s(EP) \simeq \rho_s(BP) \simeq \rho_s(FSC). \quad (31b)$$

In order to gain some quantitative insight into the above relations we have calculated and listed the values I_b (I_σ) of the baryon (σ -meson) sp impurity factor in Tables 2 and 3. In fact, the small values of I_σ also explain why it is not important to require self-consistency in the meson propagators. One observes that the difference between the results of schemes PEP and EP is small and PEP seems a quite good approximation to FSC with respect to all the hadron propagators considered. To ascertain this we have further calculated

$$\begin{aligned} F(\pm) &\equiv \langle iG(k) \rangle_\pm = u_\pm^+(ks) iG(k) u_\pm(ks) \\ &= \frac{1+a(k^2)}{D(k^2)} \left[\frac{1+b(k^2)}{1+a(k^2)} \pm \frac{k_0}{E_k} \right] M_t \end{aligned} \quad , \quad (32)$$

[8], where $+(-)$ refers to the eigenspinor of Eq. (17) with eigenvalue $+(-)E_k = [M_t^2 + \vec{k}^2]^{\frac{1}{2}}$. In Fig. 5 we have only plotted $F_{r(i)}(FSC) = Re(Im)\langle iG(FSC) \rangle_+$, with $k_0 = \sqrt{350} fm^{-1}$, since the numerical results of the three schemes P, PEP and FSC are nearly the same. Thus, if we use Eq. (32) as a criterion, we note that even $G(P)$ is a good approximation. The poles of $G(k)$ and $\Delta_\lambda(k)$ are given by the roots k^2 of $D(k^2)$ of Eq. (26c) with $a_v = b_v = 0$ and

$$D_\lambda(k^2) = k^2 + m_\lambda^2 + i\Pi_\lambda(k^2), \quad (33)$$

respectively. The ghost poles found are listed in Table 4. They are given in units of fm^{-2} .

Now let us consider the $\sigma - \omega$ model. Here we shall only present the numerical results for $\bar{g}_s^2 = 0.5263$ and $\bar{g}_v^2 \equiv \frac{g_v^2}{8\pi^2} = 1.3685$, as qualitatively they are quite typical. In Figs. 6 and 7 we have plotted the numerical results for (a_s, b_s) and (a_v, b_v) . It is seen that before $k^2 \simeq -120fm^{-2}$ the effects of self-consistency is insignificant. Hereafter they seem to become more important, but they are not large enough to cause any palpable effects on α and β . The results obtained from the five schemes nearly coincide with each other as shown in Fig. 8, where only two are drawn explicitly, because the other four are not distinguishable in the figure. Thus, in this case no self-consistent requirement is needed, just as found in Ref. [4] for the $\pi - \omega$ model. Comparing Figs. 6 and 7 with Fig. 2 one notes that $a_s(k^2)$ and $b_s(k^2)$ only change slightly due to the presence of ω mesons. However, there is a quite large difference between (a_s, b_s) and (a, b) where $a = a_s + a_v$ and $b = b_s + b_v$. This explains why Fig. 8 differs from Fig. 3 so greatly. A comparison between Figs. 3 and 8 suggests that there exists a cancellation between the effects on self-consistency due to the σ and ω mesons. This is obviously related to the σ -baryon and ω -baryon interactions and thus also to the different characteristic features contributed to the baryon-baryon interaction by the σ and ω mesons individually. It seems that these features are not only of importance to the nuclear binding and saturation, but also to the formation of baryonic excited states (see below). We expect the above relation between the cancellation and the different characteristics of meson-baryon interactions may hold generally, though the details of its regularity will depend on the participating meson fields and there may even be enhancement if their characteristics are of the same kind (which is actually defined by the 'enhancement'). If the regularity of cancellation can be extended to the case of finite density, it will be very useful, because the analysis and the renormalized calculation will be greatly simplified, when the effect of self-consistency is negligible. However, this is still a problem to be studied. To illustrate how the ω meson affects the disappearance of the effect of self-consistency we have drawn a set of α and β calculated for an intermediate $\bar{g}_v^2 = 0.3400$ in Fig. 9. We note that owing to the presence of ω mesons the maximum of each baryon spectral function becomes sharper and more distinct. Since $\alpha(k^2)$ relates directly to the probability of occurrence of an excited baryon state, it indicates that the contribution of ω mesons enhances the possibility of forming a resonant baryon state, though we do not expect that the $\sigma - \omega$ model may explain the experimentally observed baryon spectrum. From Fig. 10 it looks that a discernible effect of self-consistency exists for mesons. However, we observe

from the same figure that schemes PEP and FSC yield almost the same result. This says that the above effect can be taken account of by simply substituting $G(k; P)$ in Eqs. (8) and (10) without considering a self-consistent calculation. BEKW [4] found that for the $\pi-\omega$ model the self-consistency decreases $\rho_\pi(k^2)$, while increases $\rho_\omega(k^2)$. Owing to the difference in models, our calculation shows that the self-consistency decreases both $\rho_s(k^2)$ and $\rho_v(k^2)$. Further we note that the self-consistency and additional contribution of ω mesons still cannot eliminate the ghost poles, whose values found for the relevant hadron propagators are respectively, for baryon: $149.4215 \pm i96.8997$, for σ meson: 274.4833 and for ω meson: $178.5431(fm^{-2})$.

4 . Effects of vertex corrections on ghost poles

The principal aim of this section is to study the effects of vertex corrections on ghost poles and their elimination. For our purpose we shall only consider phenomenological form factors, though they still suffer the not yet resolved problem of violating the Ward-Takahashi identity as emphasized in Refs. [3, 7]. The vertices included in Eq. (1) are illustrated in Fig. 11, where 1 and 2 denote baryons, while λ a σ or ω meson. Phenomenologically the vertex functions may be written approximately as [14]

$$\Gamma_s(p_1, p_2, p_s) = F_b(p_1)F_b(p_2)F_s(p_s), \quad (34a)$$

$$\Gamma_\mu(p_1, p_2, p_v) = \gamma_\mu F_b(p_1)F_b(p_2)F_v(p_v), \quad (34b)$$

where F_b in Γ_s and Γ_μ will be chosen the same. Substituting Eq. (34) in Eqs. (6, 8, 10), we obtain

$$\Sigma_s^f(k) = -g_s^2 F_b(k) \int \frac{d^r q}{(2\pi)^4} F_b(q) F_s(k-q) G(q) \Delta_s(k-q), \quad (35a)$$

$$\Sigma_v^f(k) = g_v^2 F_b(k) \int \frac{d^r q}{(2\pi)^4} F_b(q) F_v(k-q) \gamma_\mu G(q) D_{\mu\nu}(k-q) \gamma_\nu, \quad (35b)$$

$$\Pi_s^f(k) = g_s^2 F_s(k) \int \frac{d^r q}{(2\pi)^4} F_b(k+q) F_b(q) Tr[G(k+q)G(q)], \quad (36)$$

$$\Pi_{\mu\nu}^f(k) = -g_v^2 F_v(k) \int \frac{d^r q}{(2\pi)^4} F_b(k+q) F_b(q) Tr[\gamma_\mu G(k+q) \gamma_\nu G(q)], \quad (37)$$

where the superscript f indicates that form factors are inserted.

In the previous section it has been shown that all the calculated renormalized hadron propagators possess ghost poles. Just as found in Refs. [4, 6, 7, 9], our calculation also shows that the ghost poles can be eliminated by a proper treatment of vertex corrections. In order to make the change of the k -dependence of the self-energies caused by them appear in a clearer form, we shall choose the form factors as simple as possible. We shall set $F_b = 1$ and

$$F_\lambda(p) = \frac{\Lambda_\lambda^2 - m_\lambda^2}{\Lambda_\lambda^2 + p^2 - i\epsilon}, \quad \lambda = s \text{ or } v \quad (38)$$

where $\epsilon \rightarrow 0^+$ indicates the displacement of the poles. From Eq. (35) it is immediately seen that $\Sigma_\lambda^f(\lambda = s \text{ or } v)$ are made finite by this choice. However, according to Eqs. (36) and (37) we have

$$\Pi_s^f(k) = F_s(k)g_s^2 \int \frac{d^4 q}{(2\pi)^4} Tr[G(k+q)G(q)] \equiv F_s(k)\widehat{\Pi}_s(k), \quad (39)$$

$$\Pi_{\mu\nu}^f(k) = -F_v(k)g_v^2 \int \frac{d^4 q}{(2\pi)^4} Tr[\gamma_\mu G(k+q)\gamma_\nu G(q)] \equiv F_v(k)\widehat{\Pi}_{\mu\nu}(k), \quad (40)$$

where $\widehat{\Pi}_s$ ($\widehat{\Pi}_{\mu\nu}$) is just the integral in Eq. (8) (Eq. (10)) with $\Gamma_s = 1$ ($\Gamma_\nu = \gamma_\nu$). Both of them are divergent. As no confusion will arise, the bar over $\Pi_{\mu\nu}$ will hereafter be omitted. In order to investigate the effect of the multiplicative factor F_λ on the elimination of ghost poles, we shall, just as Ref. [6], substitute the renormalized Π_s and $\Pi_{\mu\nu}$ for $\widehat{\Pi}_s$ and $\widehat{\Pi}_{\mu\nu}$, respectively. The explicit expressions of $\Pi_{\mu\nu}$ and Π_s have been given in Eqs. (11, 12, 28, 29).

Now let us consider the baryon self-energy. Substituting Eq. (38) into Eq. (35) and using the method of integral parameterization, we get

$$\begin{aligned} \Sigma_s^f(k) &= -2ig_s^2 \int \int d\sigma^2 dm^2 (\Lambda_s^2 - m_s^2) h_s(-m^2) \\ &\times \int_0^1 dx \int_0^{1-x} dy \int \frac{d^4 Q}{(2\pi)^4} \frac{(x+y)\gamma_\mu k_\mu f_\alpha(-\sigma^2) + iM_t f_\beta(-\sigma^2)}{[Q^2 + L_f^2 - i\eta]^3}, \end{aligned} \quad (41a)$$

$$L_f^2 = (x+y)(1-x-y)k^2 + x\Lambda_s^2 + ym^2 + (1-x-y)\sigma^2, \quad (41b)$$

where $\eta \rightarrow 0^+$. It is seen that the Wick rotation can be applied and the four-dimensional integral can be worked out immediately. From Eqs. (22) and (41) we obtain

$$\begin{aligned} a_s^f(k) &= \frac{g_s^2}{16\pi^2} \iint_0^\infty d\sigma^2 dm^2 \int_0^1 dz \frac{(\Lambda_s^2 - m_s^2)}{(\Lambda_s^2 - m_s^2)} z \\ &\times f_\alpha(-\sigma^2) h_s(-m^2) \ln \frac{L_f^2(z, z, \sigma^2, m^2, k^2)}{L_f^2(0, z, \sigma^2, m^2, k^2)}, \end{aligned} \quad (42a)$$

$$\begin{aligned} b_s^f(k) &= \frac{g_s^2}{16\pi^2} \frac{M_t}{M} \iint_0^\infty d\sigma^2 dm^2 \int_0^1 dz \frac{(\Lambda_s^2 - m_s^2)}{(\Lambda_s^2 - m_s^2)} \\ &\times f_\beta(-\sigma^2) h_s(-m^2) \ln \frac{L_f^2(0, z, \sigma^2, m^2, k^2)}{L_f^2(z, z, \sigma^2, m^2, k^2)}, \end{aligned} \quad (42b)$$

$$L_f^2(x, z, \sigma^2, m^2, k^2) = z(1-z)k^2 + (1-z)\sigma^2 + zm^2 + x(\Lambda_s^2 - m^2). \quad (42c)$$

According to Eq. (42c) $L_f^2(z, z, \sigma^2, m^2, k^2)$ is independent of m^2 and in the neighbourhood of $m^2 = \Lambda_s^2$

$$\ln \frac{L_f^2(0, z, \sigma^2, m^2, k^2)}{L_f^2(z, z, \sigma^2, m^2, k^2)} = \frac{z}{L_f^2(z, z, \sigma^2, m^2, k^2)}(m^2 - \Lambda_s^2) + \dots, \quad (43)$$

thus the integrand is well behaved at $m^2 = \Lambda_s^2$ even if $\Lambda_s^2 > th_s$. Similarly from Eq. (41)

$$a_v^f(k) = \frac{g_v^2}{8\pi^2} \iint_0^\infty d\sigma^2 dm^2 \int_0^1 dz \frac{(\Lambda_v^2 - m_v^2)}{(\Lambda_v^2 - m^2)} z \times f_\alpha(-\sigma^2) h_v(-m^2) \ln \frac{L_f^2(z, z, \sigma^2, m^2, k^2)}{L_f^2(0, z, \sigma^2, m^2, k^2)}, \quad (44a)$$

$$b_v^f(k) = \frac{g_v^2}{4\pi^2} \frac{M_t}{M} \iint_0^\infty d\sigma^2 dm^2 \int_0^1 dz \frac{(\Lambda_v^2 - m_v^2)}{(\Lambda_v^2 - m^2)} \times f_\beta(-\sigma^2) h_v(-m^2) \ln \frac{L_f^2(z, z, \sigma^2, m^2, k^2)}{L_f^2(0, z, \sigma^2, m^2, k^2)}. \quad (44b)$$

Eqs. (42) and (44) combined with Eqs. (23, 26, and 28-30) build a closed set, which has been solved by iteration. However, one notes that instead of Eqs.(26b and c) one should now write

$$\beta(k^2) = \frac{M}{\pi M_t} Im \left[\frac{1 + b_s(k^2) + b_v(k^2)}{D(k^2)} \right], \quad (26d)$$

$$D(k^2) = (1 + a_s(k^2) + a_v(k^2))^2 k^2 + (1 + b_s(k^2) + b_v(k^2))^2 M^2, \quad (26e)$$

while between M_t and M we have

$$(1 + a_s(-M_t^2) + a_v(-M_t^2))^2 M_t^2 = (1 + b_s(-M_t^2) + b_v(-M_t^2))^2 M^2. \quad (27)$$

The numerical results are represented graphically in Fig. 12 to 15 for $\Lambda_s = \Lambda_v = 5.0676 fm^{-1}(1GeV)$. The other parameters are the same as chosen previously. According to our calculation no noticeable difference between scheme BP and FSC exists, thus only the latter is plotted. From the figures it is seen that the self-consistency is almost of no effect. Comparing Figs. 12-13 with Figs. 6-7 one notes that the two set of (a, b) differ significantly, especially with respect to their asymptotic behavior. However, the results given in Figs. 8 (10) and 14 (15) for the baryon (meson) spectral functions are qualitatively similar. In Table 5 we have presented the values of I_b and I_λ calculated according to the method of renormalization and of form factors. If we adjust the parameters, it is possible to make the two

sets approach each other better. This suggests that for the calculation of hadron propagators the two methods can yield closely approximated results. We have found that all the ghost poles are eliminated. The reason seems intimately related with the change of the asymptotic behavior caused by the vertex correction. For the baryon self-energy we see that as $|k^2| \rightarrow \infty$, the Log-function $|\ln[K^2(-M_t^2)/K^2(k^2)]| \rightarrow \infty$ in Eqs. (24, 25), while in Eqs. (42, 44) we have $|\ln[L_f^2(z, z, \sigma^2, m^2, k^2)/L_f^2(0, z, \sigma^2, m^2, k^2)]| \rightarrow 0$. This fact also explains the asymptotic behavior mentioned above. As shown in Eqs. (39, 40) the meson self-energies Π_λ^f are obtained by simply multiplying the corresponding expressions given in Section 2 by $F_\lambda(k^2)$, which tends to $|k^2|^{-1}$ as $|k^2| \rightarrow \infty$. From Fig. 16 and Eqs. (28, 29) one sees that $i\Pi_\lambda(k^2)$ bends the straight line $k^2 + m_\lambda^2$ to intersect the abscissa axis (k^2 -axis) and thus $\Delta_\lambda(k)$ gets a ghost pole. However no such bending will be induced by $i\Pi_\lambda^f = F_\lambda(k^2)i\Pi_\lambda(k^2)$ as shown in Fig. 17, because if k^2 becomes large, $i\Pi_\lambda^f$ will be negligible compared with k^2 . It is interesting to note that there will be no ghost poles if $i\Pi_\lambda(k^2)$ bends the straight line upward or the curve $D_\lambda = D_\lambda(k^2)$ turns upward before it intersects the k^2 -axis.

5 . Concluding remarks

Under the self-consistent HF approximation we have solved the coupled set of DS equations for the renormalized hadron propagators in the $\sigma - \omega$ model. Since this set can be solved rigorously, it provides a convenient means for the study of the effects of self-consistency. Our calculation shows that in the case of zero-density scheme PEP gives a quite good approximation to the FSC scheme and there is no need to require self-consistency in the meson propagators. In the $\sigma - \omega$ case the self-consistency almost has no effect on the baryon propagator, since there is a cancellation between the effects caused by the two kinds of mesons, whereas for the σ case a FSC calculation is also unnecessary, because the iteration procedure converges quickly if an appropriate initial input is chosen. Fig. 3 shows that the self-consistency diminishes the continuum part of the baryon spectral representation predicted by scheme P. From Tab. 2 one observes that this part is by no means always unimportant. However, there is generally no need to consider scheme BP, since if scheme P does not yield a good enough result, one may go one step further to use scheme PEP. For the study of nuclear matter and nuclear structure one has to take the case of non-zero density into account. The question whether in the latter case the above conclusions still hold remains to be studied. Using the method of phenomenological form factors, we have also investigated the significance of vertex corrections. Our calculation confirms the results of

Refs. [4, 6, 7, 9], namely the ghost poles in the hadron propagators can be eliminated by vertex functions with damping asymptotic behavior. In Ref. [7] it was found that the baryon spectral function $A_R(\kappa)$ can be negative for some values of real κ if only the coupling with ω -mesons is considered. In the latter case we have also found that $\alpha(k^2)$ may be negative in a region close to the threshold. Though, if in addition to ω other mesons are taken into account, the above problem does not occur, it still has to be studied and is being under study, because the coupling with ω -mesons is of importance and according to their definitions and physical meanings, both $A_R(\kappa)$ and $\alpha(k^2)$ should be ≥ 0 .

The work is supported in part by the National Natural Science Foundation of China and the Foundation of Chinese Education Ministry.

References

- [1] W. D. Brown, R. D. Puff and L. Wilets, *Phys. Rev. C* 2 (1970) 331.
- [2] A. F. Bielajew and B. D. Serot, *Ann. Phys.* 156 (1984) 215; A. F. Bielajew, *Nucl. Phys. A* 404 (1983) 428.
- [3] B. D. Serot and J. D. Walecka, *Adv. Nucl. Phys.* 16 (1986) 1; B. D. Serot, *Rep. Prog. Phys.* 55 (1992) 1855.
- [4] M. E. Bracco, A. Eiras, G. Krein and L. Wilets, *Phys. Rev. C* 49 (1994) 1299.
- [5] J. Milana, *Phys. Rev. C* 44 (1991) 527.
- [6] M. P. Allendes and B. D. Serot, *Phys. Rev. C* 45 (1992) 2975.
- [7] G. Krein, M. Nielsen, R. D. Puff and L. Wilets, *Phys. Rev. C* 47 (1993) 2485.
- [8] S. S. Wu, J. M. Zhu, K. Z. Liu and Y. J. Yao, *Eur. Phys. J. A* 6 (1999) 345; Y. J. Yao, H. X. Zhang, J. M. Zhu, K. Z. Liu and S. S. Wu, *Chin. Phys. Lett.* 17 (2000) 720.
- [9] C. A. da Rocha, G. Krein and L. Wilets, *Nucl. Phys. A* 616 (1997) 625.
- [10] N. M. Kroll, T. D. Lee and B. Zumino, *Phys. Rev.* 157 (1967) 1376.
- [11] D. Lurie, *Particles and fields* (Interscience, New York, 1968).
- [12] S. S. Wu, Y. J. Yao, *Eur. Phys. J. A* 3 (1998) 49.
- [13] J. D. Bjorken and S. D. Drell, *Relativistic Quantum Fields* (McGraw-Hill, New York, 1965).
- [14] B. C. Pearce and B. K. Jennings, *Nucl. Phys. A* 528 (1991) 655; F. Gross, J. W. Van Orden and K. Holinde, *Phys. Rev. C* 45 (1992) 2094.

Table

Table 1 : Different calculation schemes.

Name	$\Sigma_s (\Sigma_v)$	$\Pi_s (\Pi_v)$
P	$G_\Sigma^0, \Delta_s^0 (\Delta_v^0)$	G_Σ^0
PEP	$G(P), \Delta_s^0 (\Delta_v^0)$	$G(P)$
EP	$G(P), \Delta_s^0(P) (\Delta_v^0(P))$	$G(P)$
BP	$G(BP), \Delta_s^0 (\Delta_v^0)$	$G(BP)$
FSC	$G(FSC), \Delta_s^0(FSC) (\Delta_v^0(FSC))$	$G(FSC)$

Table 2 : Values of the baryon impurity factor I_b .

Scheme	P	PEP	EP	BP	FSC
$\bar{g}_s^2 = 0.5263$	0.4157	0.3528	0.3504	0.3672	0.3664
$\bar{g}_s^2 = 0.6517$	0.4638	0.3253	0.3227	0.3756	0.3752

Table 3 : Values of the σ -meson impurity factor I_σ .

Scheme	P	PEP	FSC
$\bar{g}_s^2 = 0.5263$	0.1725	0.1178	0.1241
$\bar{g}_s^2 = 0.6517$	0.1557	0.0931	0.1017

Table 4 : Ghost poles of the baryon and σ -meson propagators.

Propagator	Baryon	σ -meson
$\bar{g}_s^2 = 0.5263$	$35.5356 \pm i253.5311$	246.7354
$\bar{g}_s^2 = 0.6517$	$-13.6188 \pm i127.7365$	177.4338

Table 5 : Impurity factors calculated according to the method of renormalization (I) and of form factors (II).

Impurity factor	I_b	I_σ	I_ω
I	0.2905	0.1334	0.1870
II	0.2701	0.0459	0.0643

Table 1 on P₉, Tables 2-4 on P₁₀, Table 5 on P₁₄.

Figure captions

- Fig. 1** : Diagrammatic representation of the different self-consistent (dressed) HF schemes. a. the baryon propagator, b. the σ -meson propagator, c. the ω -meson propagator.
- Fig. 2** : Numerical results of (a_s, b_s) . (a) the real part, (b) the imaginary part. [$BP \simeq FSC$, \simeq means indistinguishable or almost indistinguishable.]
- Fig. 3** : The baryon spectral functions $\alpha(k^2)$ and $\beta(k^2)$. [$\alpha(BP) \simeq \alpha(FSC)$; $\alpha(PEP) \simeq \alpha(EP)$]
- Fig. 4** : The σ -meson spectral functions $\rho_s(k^2)$.
- Fig. 5** : Graphical representation for $F(+)=\langle iG(k) \rangle_+$, where $F_r = Re \langle iG_{HF}(FSC) \rangle_+$, $F_i = Im \langle iG_{HF}(FSC) \rangle_+$.
- Fig. 6** : Numerical results of a_s and a_v . (a) the real part, (b) the imaginary part. [$a_{sr}(BP) \simeq a_{sr}(FSC)$; $a_{si}(BP) \simeq a_{si}(FSC)$; $a_{vr}(BP) \simeq a_{vr}(FSC)$]
- Fig. 7** : Numerical results of b_s and b_v . (a) the real part, (b) the imaginary part. [$b_{sr}(BP) \simeq b_{sr}(FSC)$; $b_{si}(BP) \simeq b_{si}(FSC)$; $b_{vr}(BP) \simeq b_{vr}(FSC)$]
- Fig. 8** : The baryon spectral functions $\alpha(k^2)$ and $\beta(k^2)$ calculated with baryon coupling with both σ and ω meson.
- Fig. 9** : The baryon spectral functions $\alpha(k^2)$ and $\beta(k^2)$ for $\bar{g}_v^2 = 0.34$.
- Fig. 10** : The meson spectral functions $\rho_\lambda(k^2)$. (a) σ -meson: $\lambda = \sigma$; (b) ω -meson: $\lambda = \omega$. [$PEP \simeq FSC$]
- Fig. 11** : The baryon-meson vertices.
- Fig. 12** : Numerical results of (a_s, a_v) [FF]. where the square bracket [FF] indicates that the results are obtained by the method of form factors.
- Fig. 13** : Numerical results of (b_s, b_v) [FF].
- Fig. 14** : The baryon spectral functions $\alpha(k^2)$ and $\beta(k^2)$.
- Fig. 15** : The meson spectral functions $\rho_\lambda(k^2)$ [FF]. (a) σ -meson: $\lambda = \sigma$; (b) ω -meson: $\lambda = \omega$.

Fig. 16 : Plot of $D_\lambda = D_\lambda(k^2)$ versus k^2 . (a) σ -meson: $\lambda = s$; (b) ω -meson: $\lambda = \omega$.

Fig. 17 : The same as Fig. 16 but calculated by the method of form factors.

Fig. 1 on P₂, Figs. 2-4 on P₉, Figs. 5-7 on P₁₀, Figs. 8-10 on P₁₁, Figs. 12-17 on P₁₄.

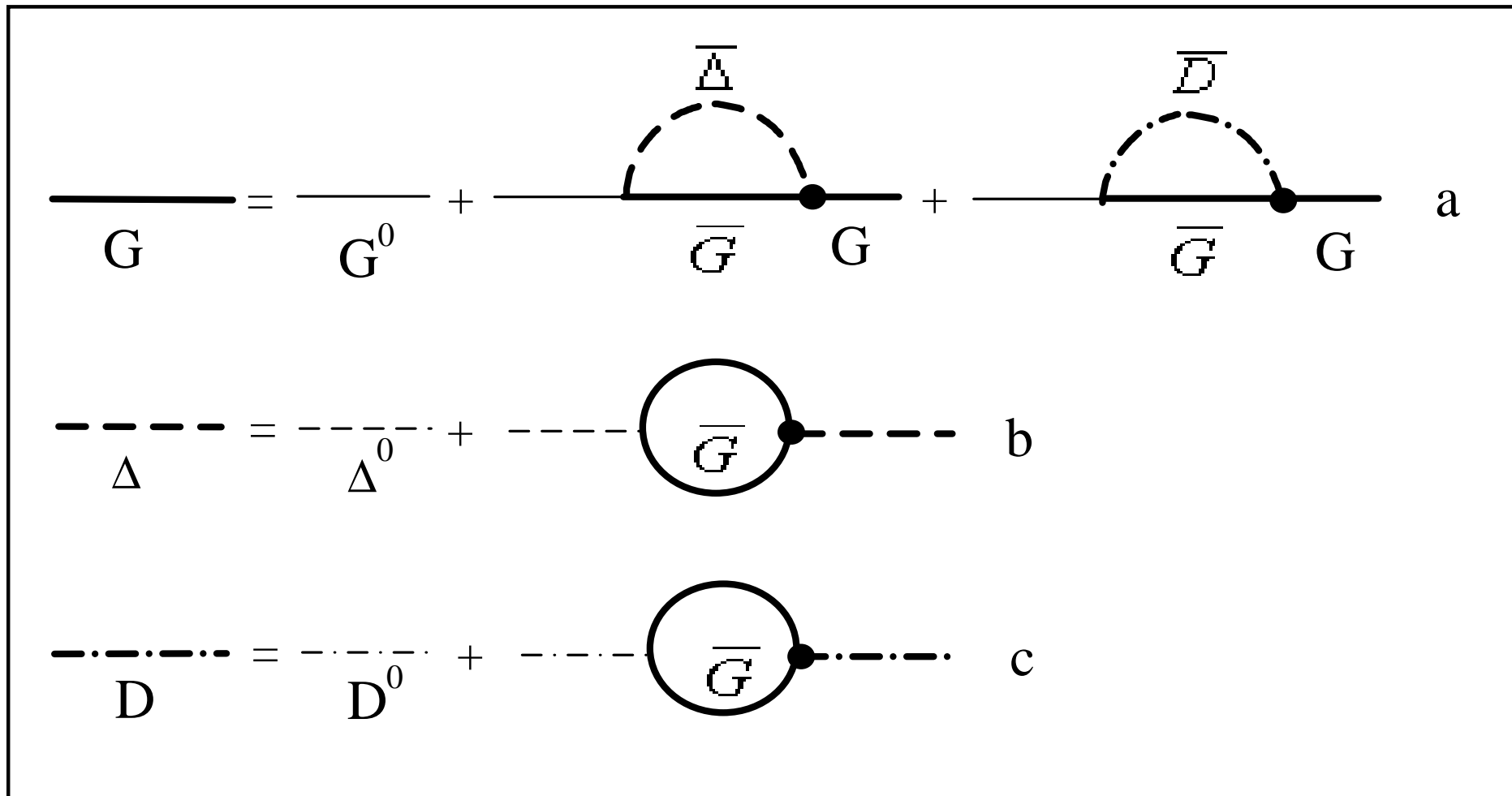


Fig. 1

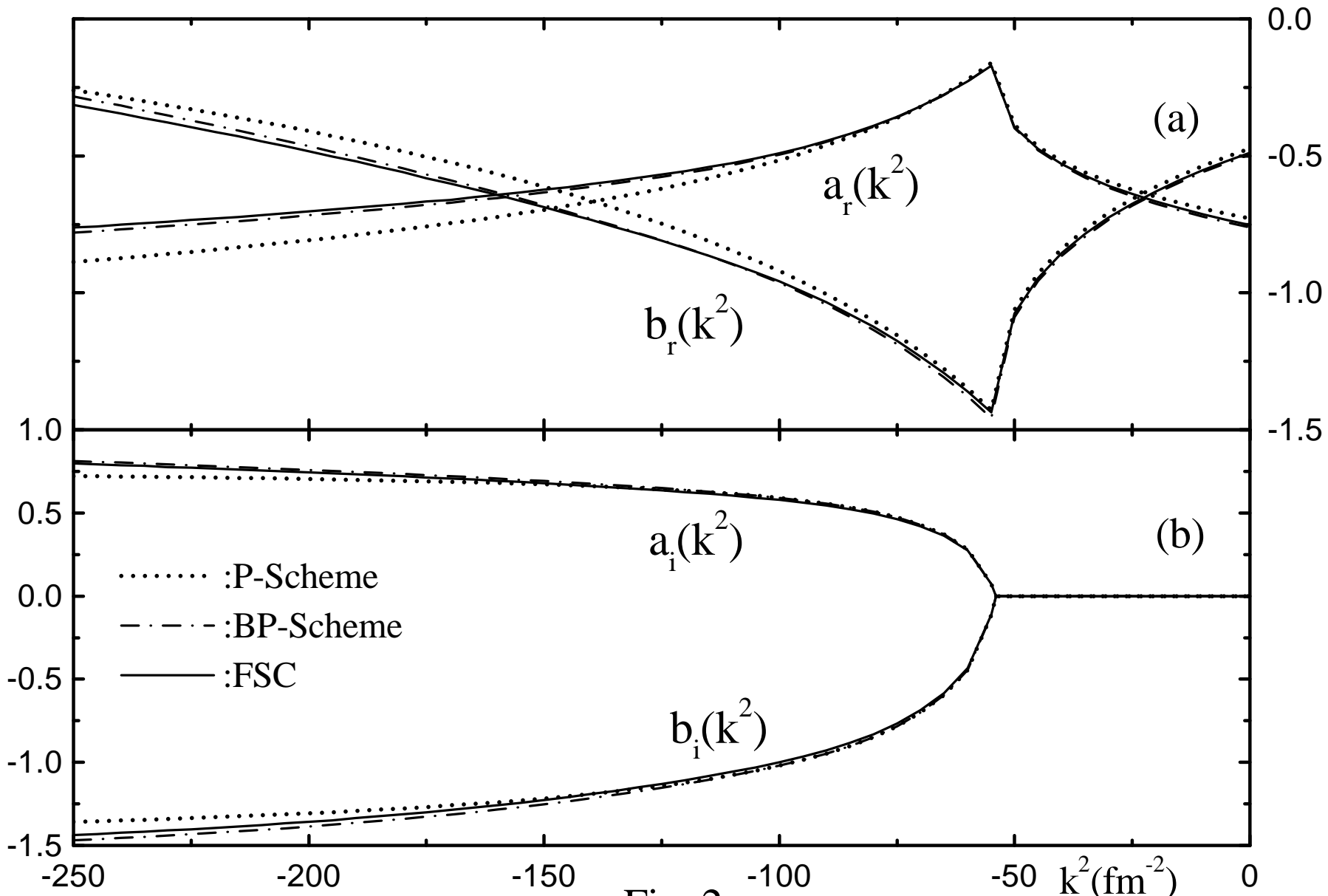


Fig. 2

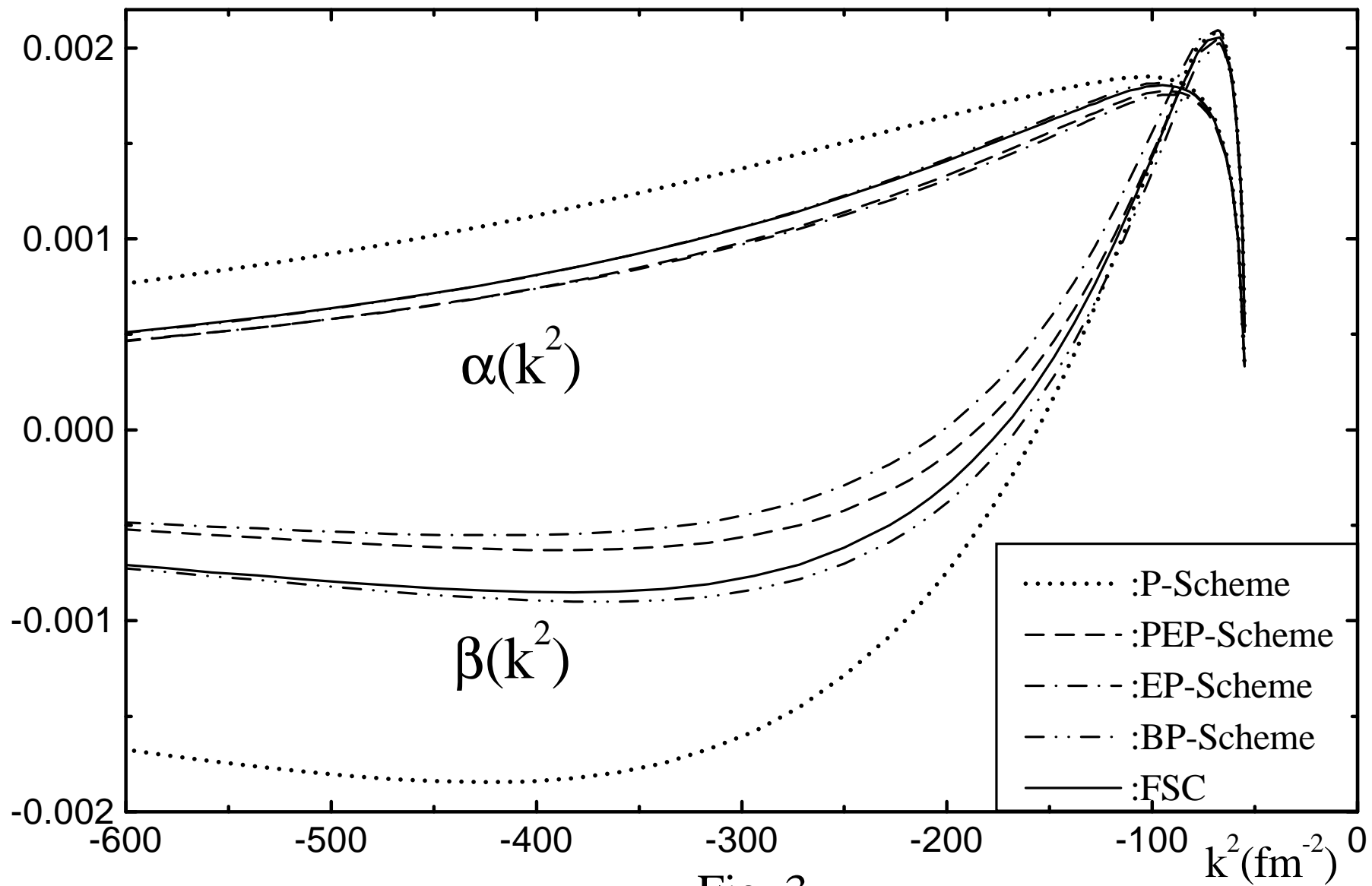


Fig. 3

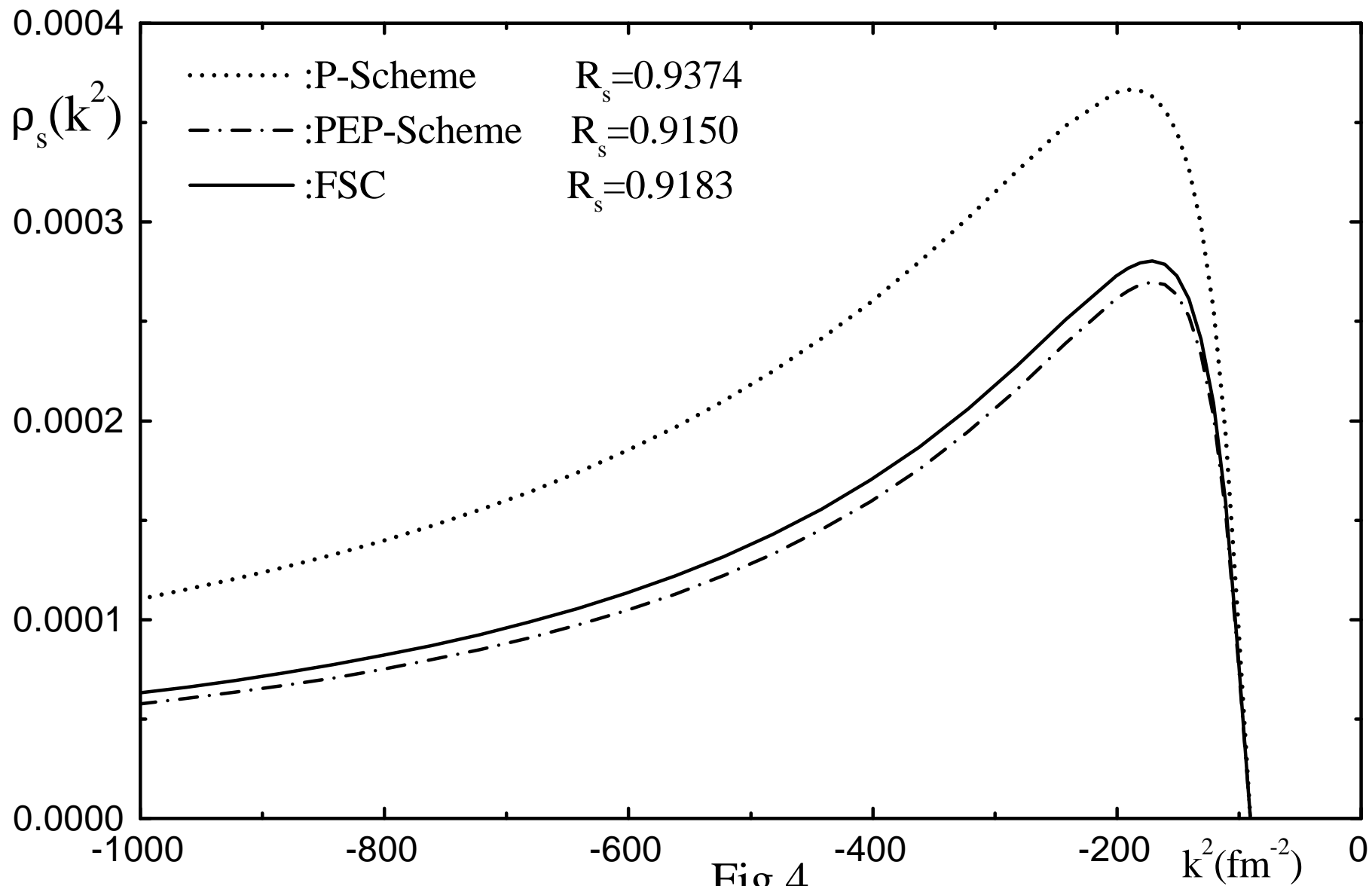


Fig.4

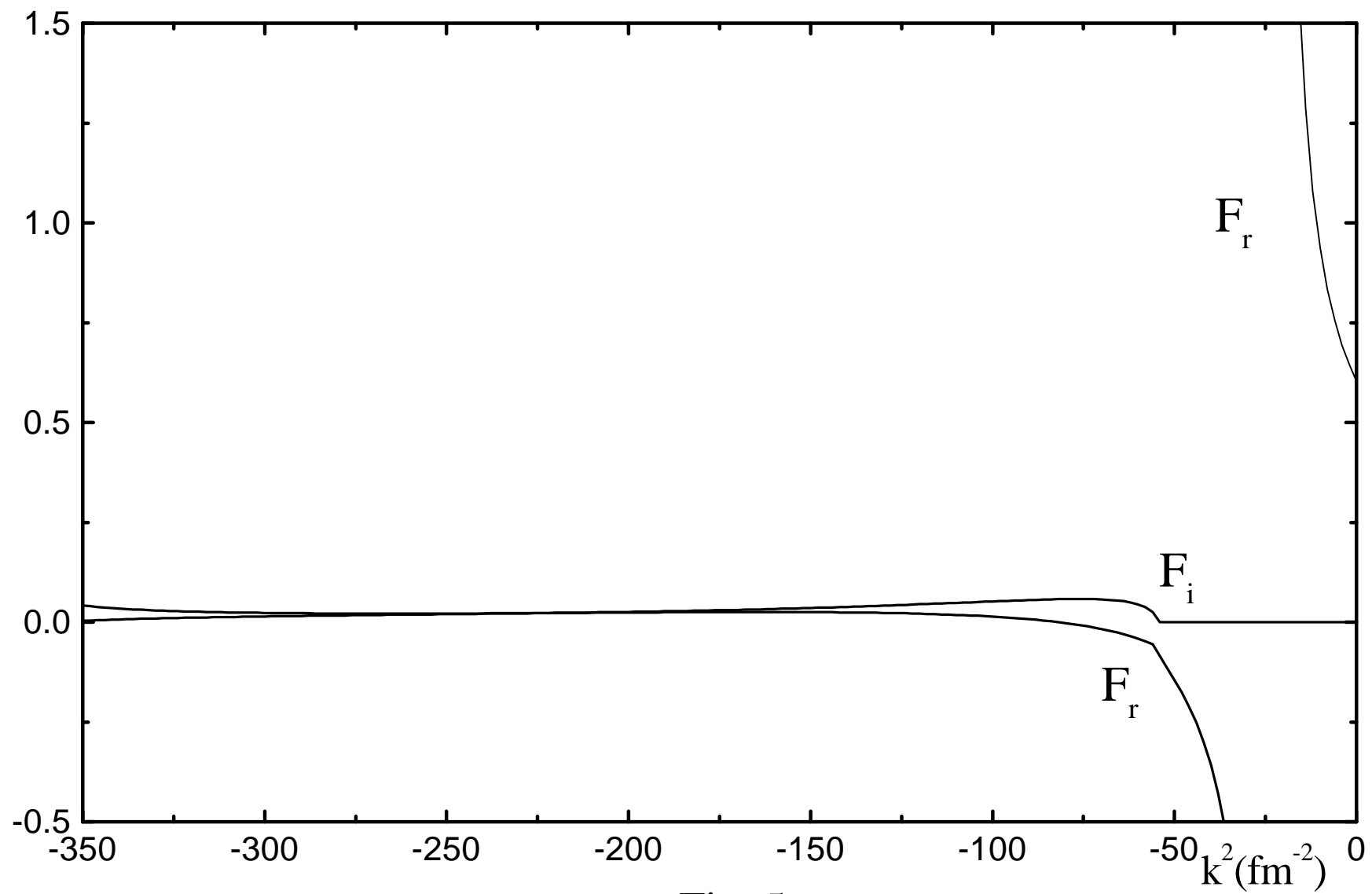


Fig. 5

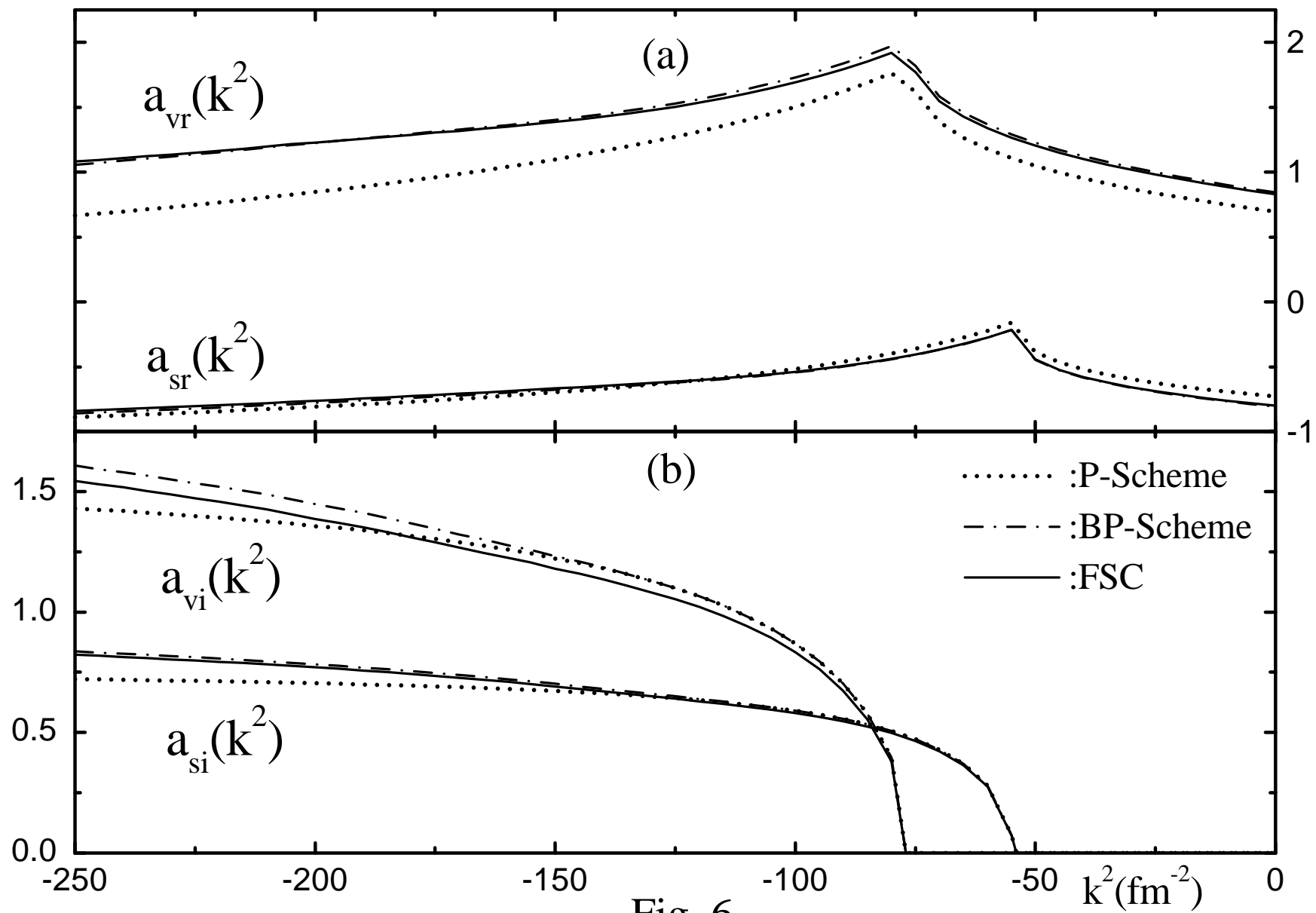


Fig. 6

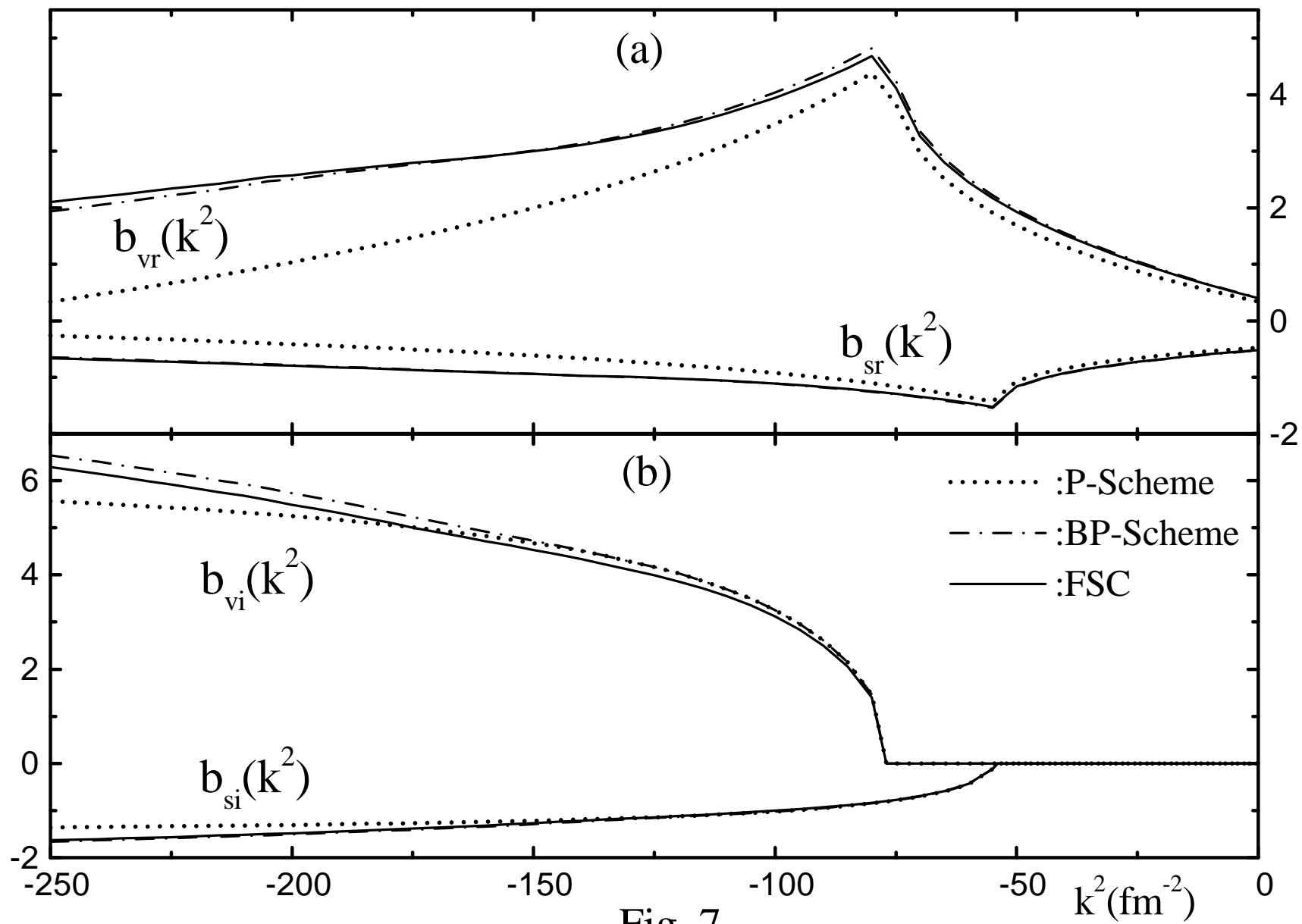


Fig. 7

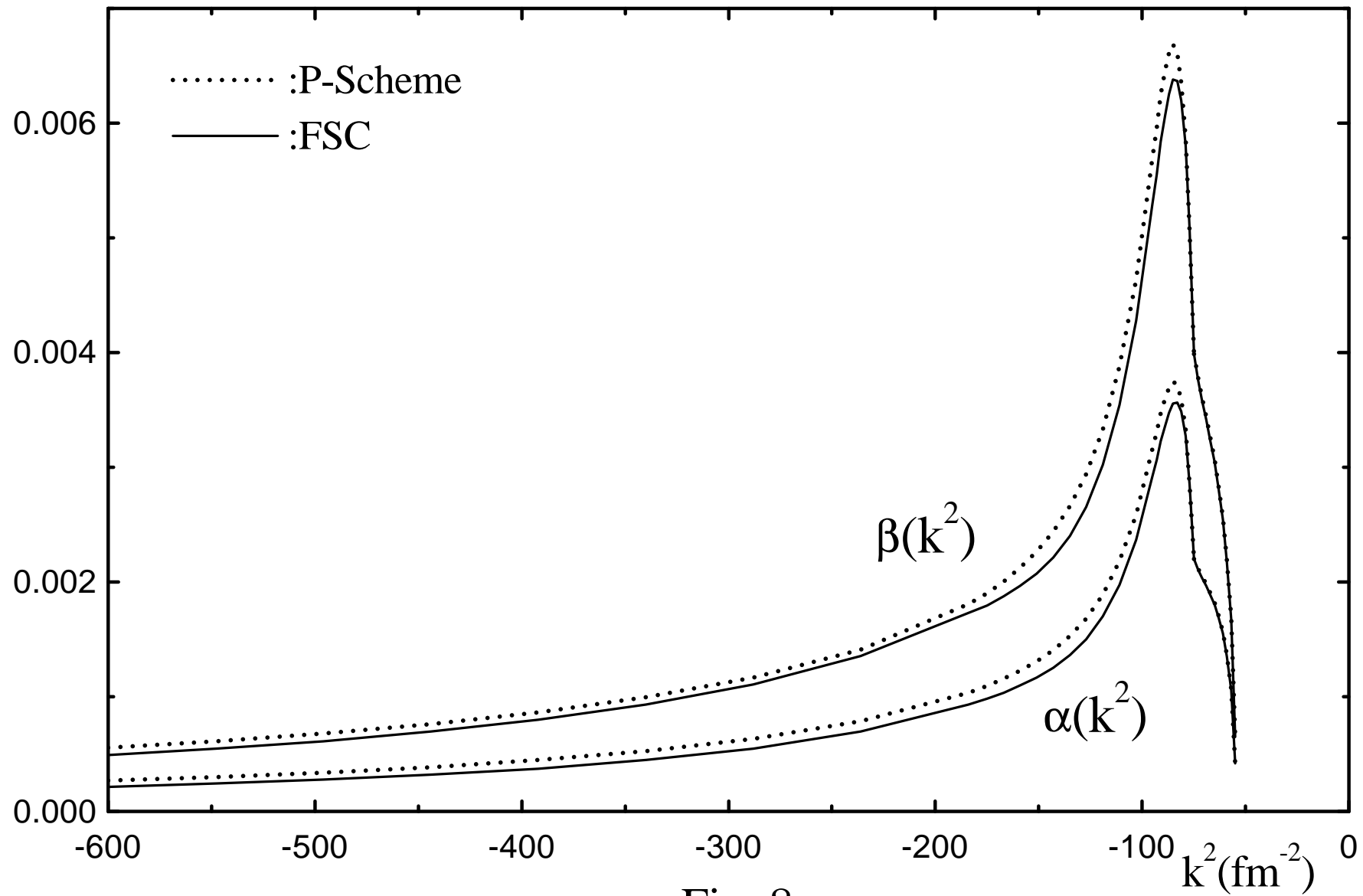


Fig. 8

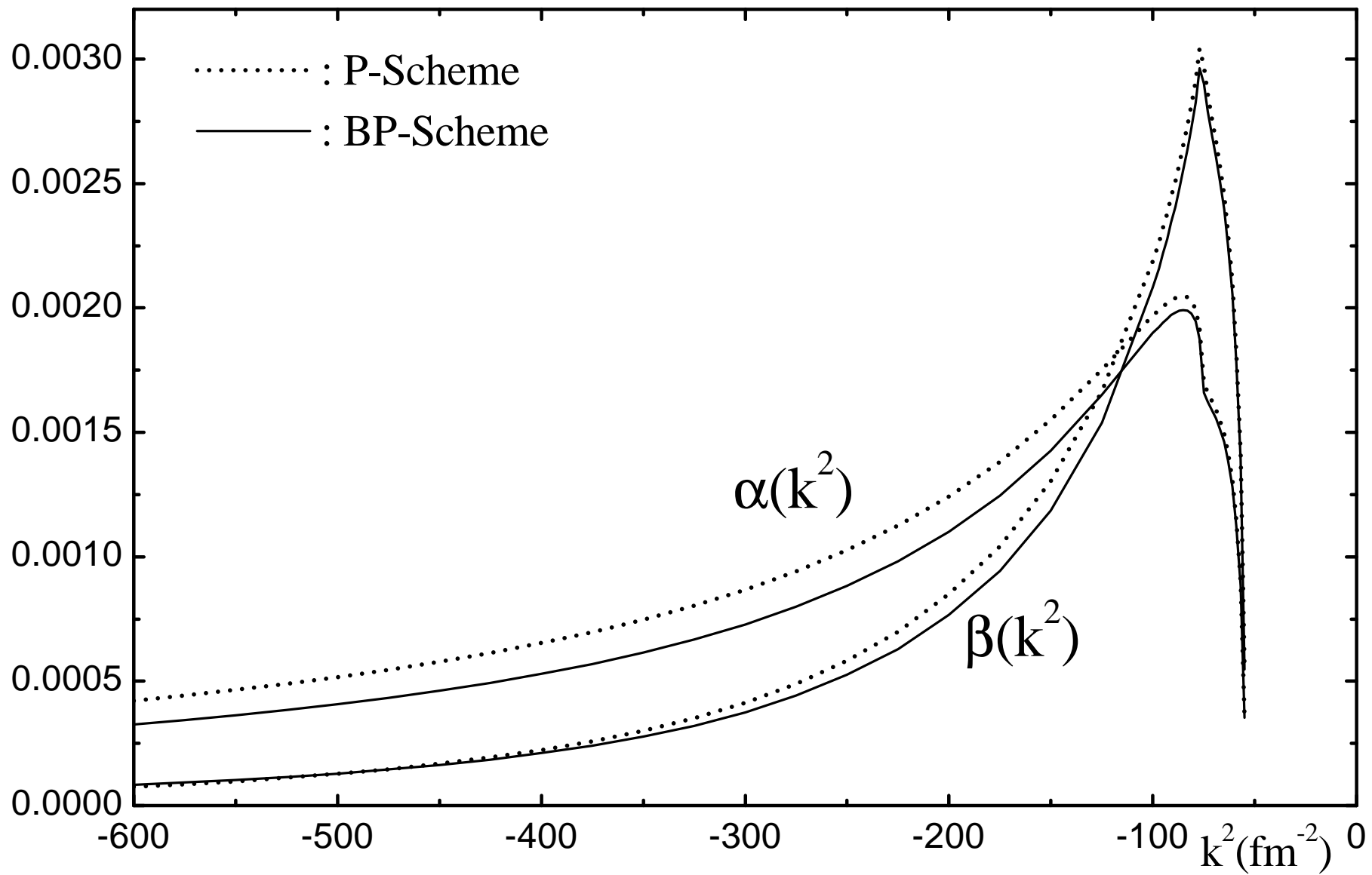


Fig. 9

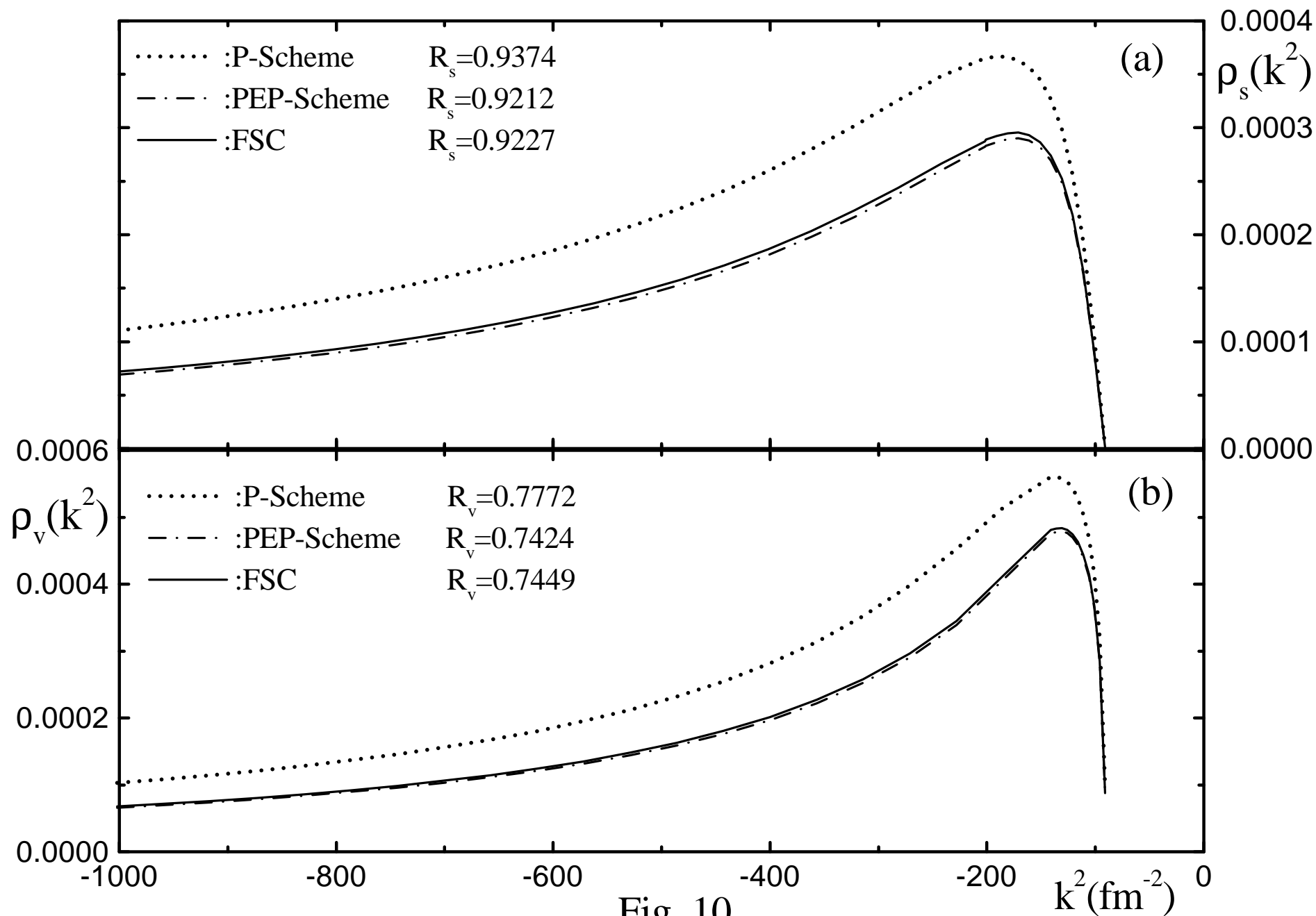


Fig. 10

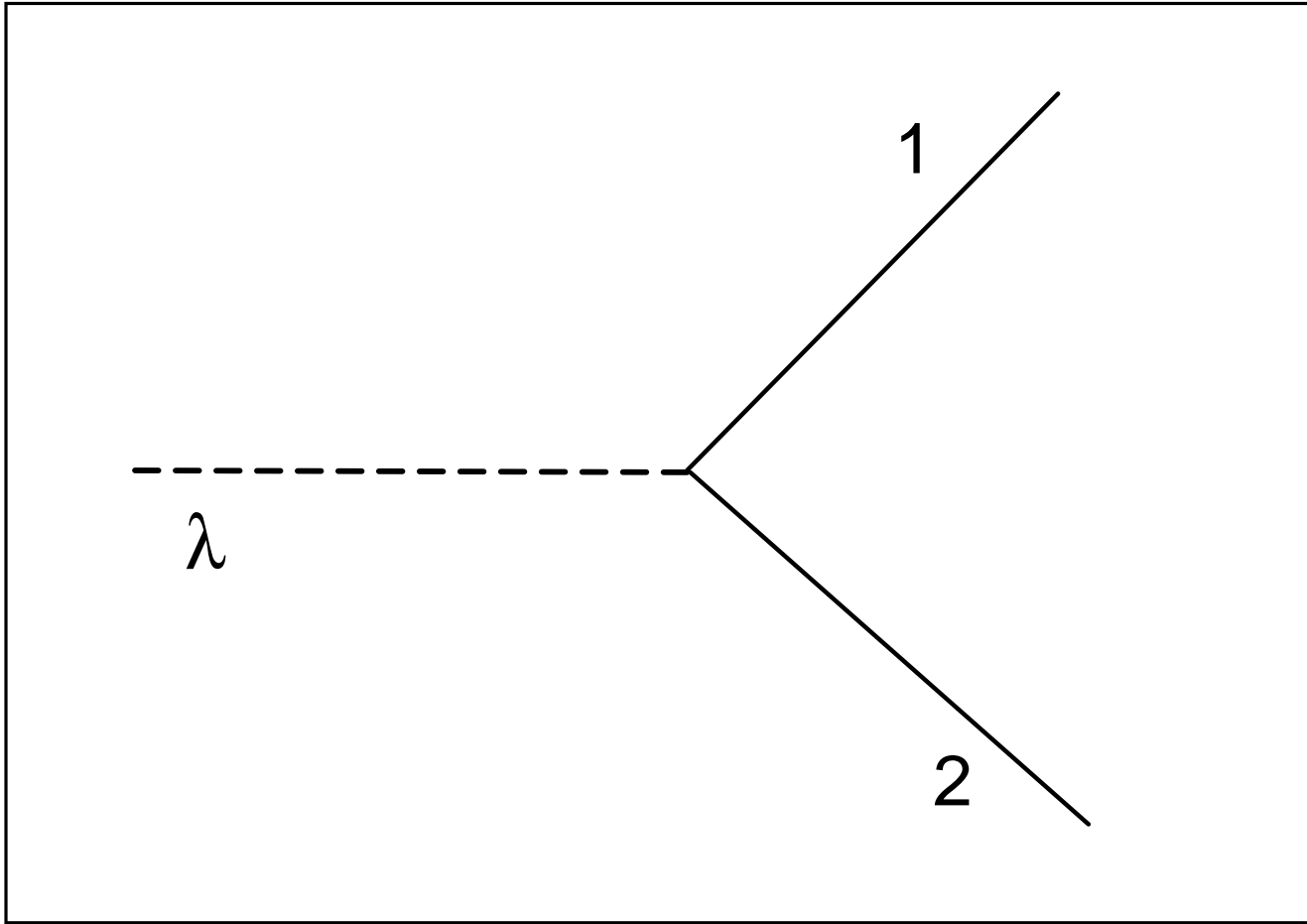


Fig. 11

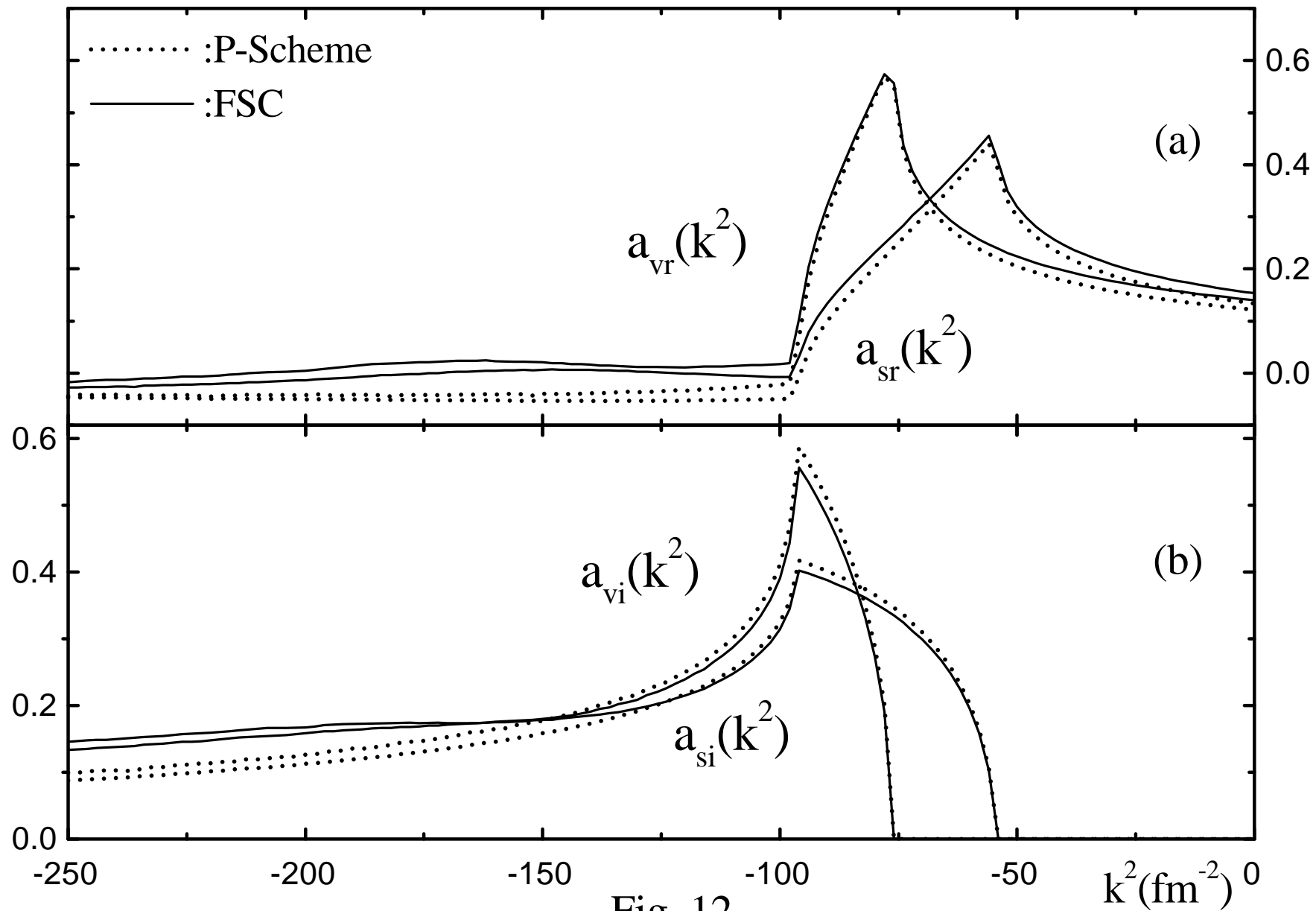


Fig. 12

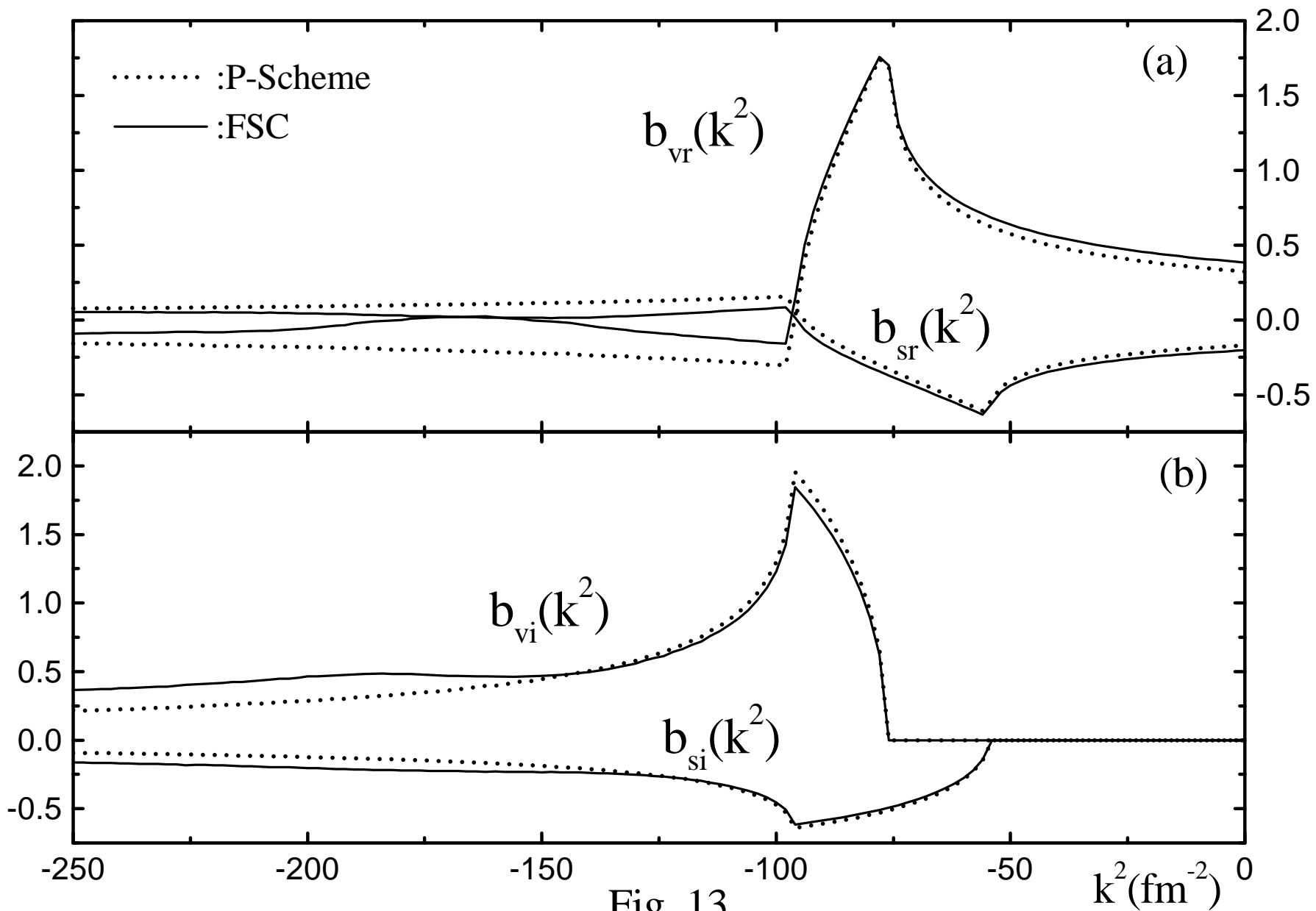


Fig. 13

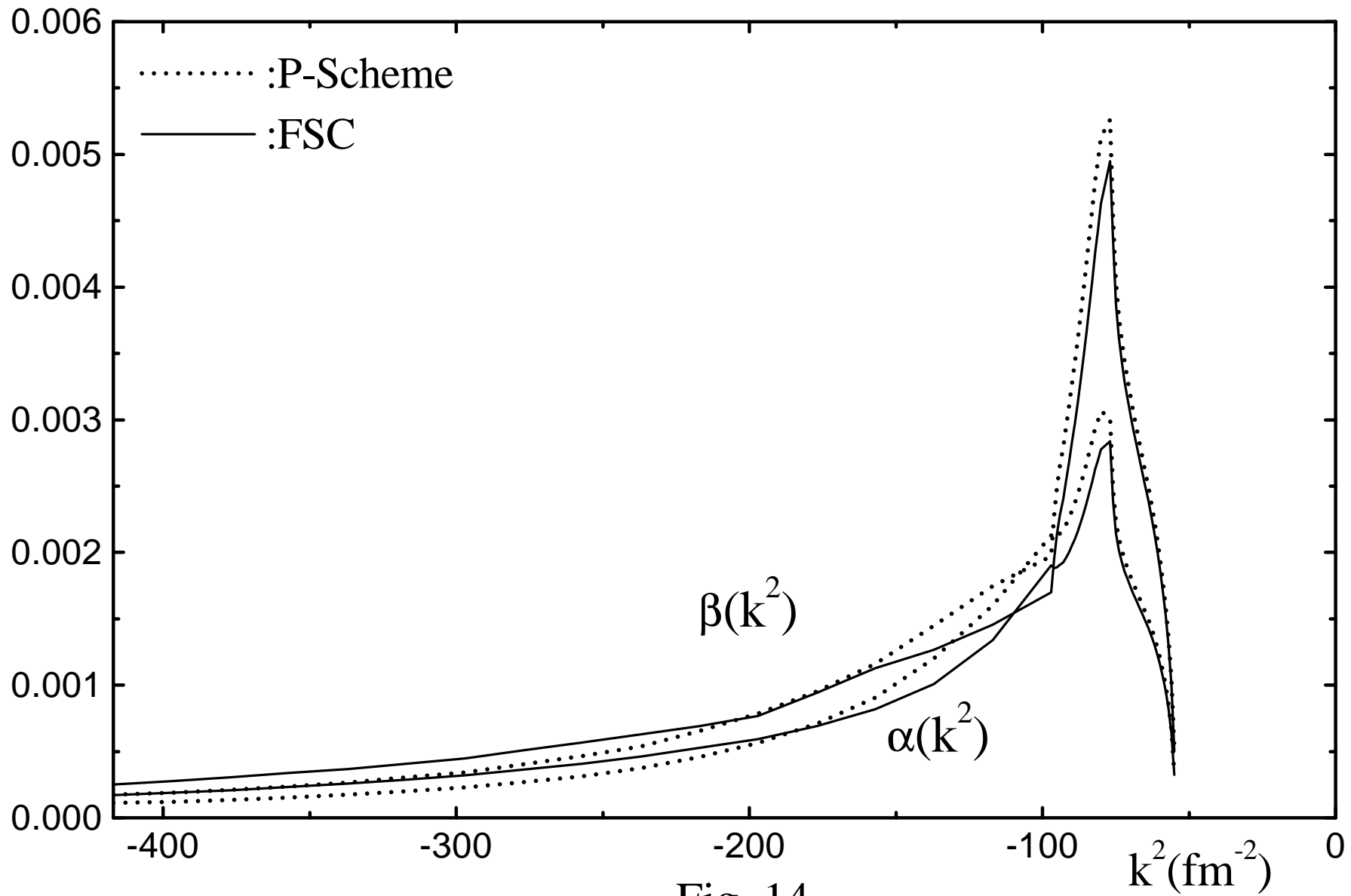


Fig. 14

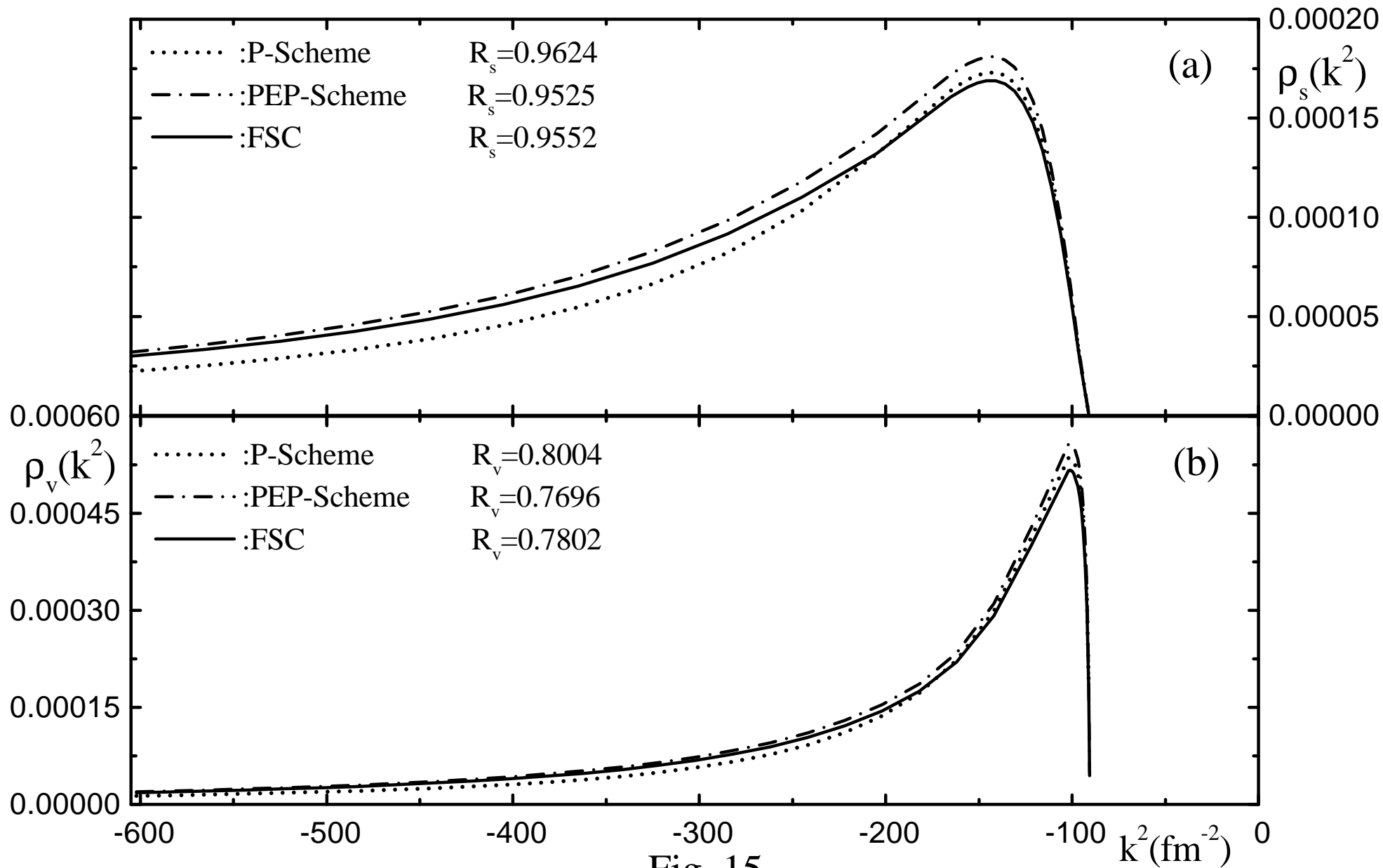


Fig. 15

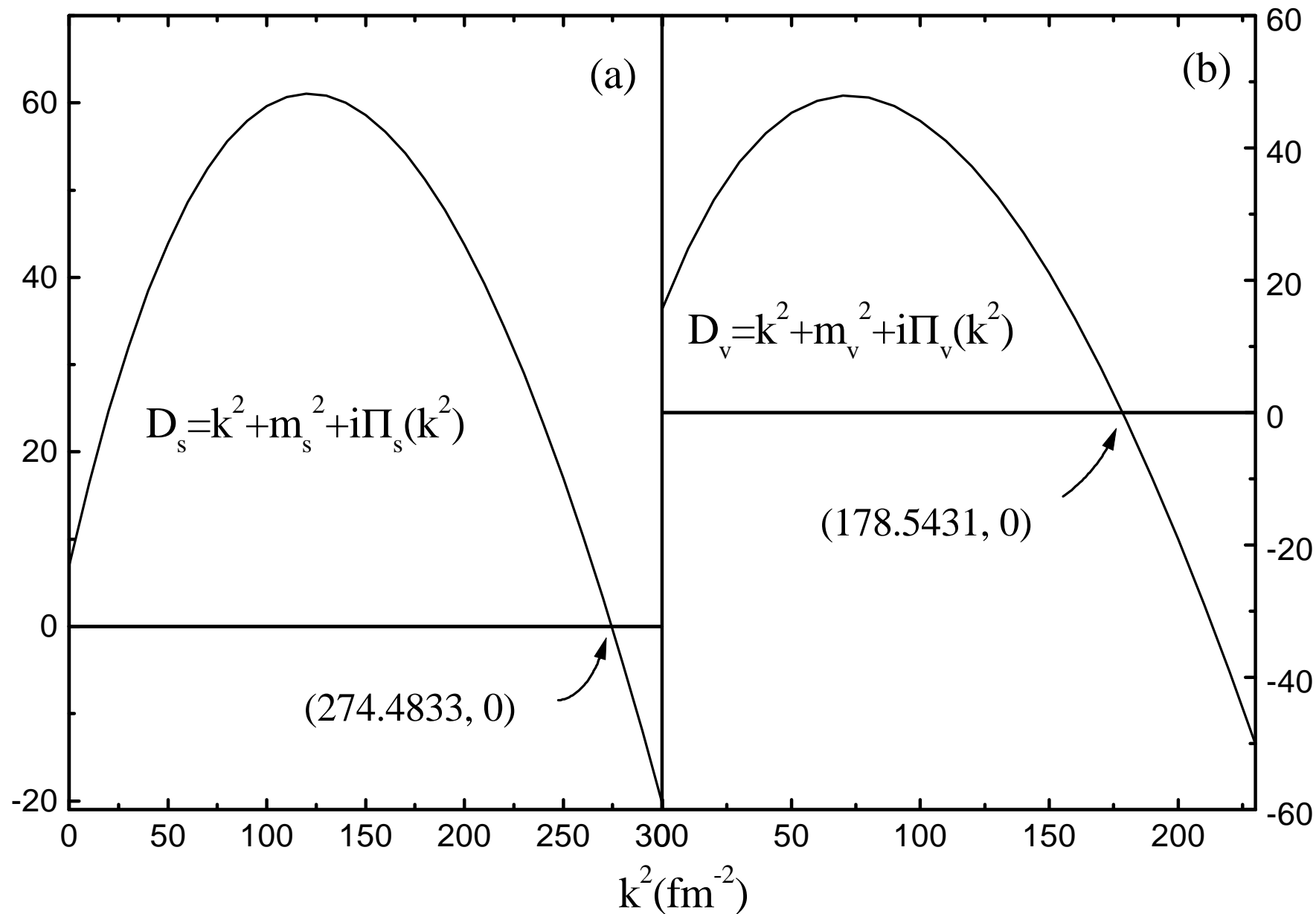


Fig. 16

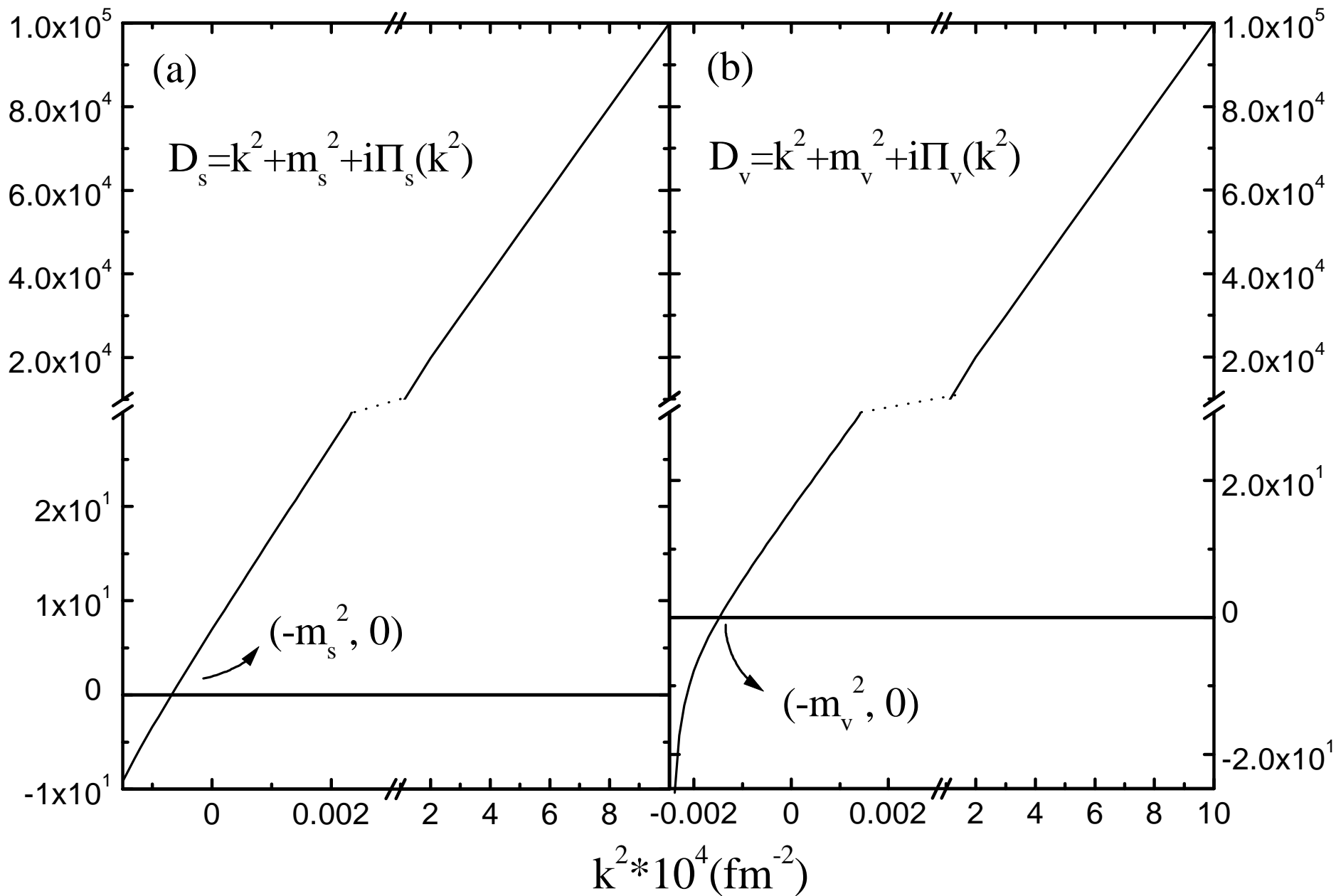


Fig. 17